

**MEASUREMENT OF LOWER ORDER ABERRATIONS IN THE EYE USING
WAVEFRONT ABERROMETRY BASED ON A CCD CAMERA**

A Project Study Presented to the Faculty of
Electronics Engineering Department
College of Engineering
Technological University of the Philippines

In Partial Fulfilment of the Course Requirements for the Degree of
Bachelor of Science in Electronics Engineering

Submitted by:
Atas, Marie Cattleah D.
Landicho, Larish Mariam T.
Lobo, Abigail D.
Orubia, Carla Joy L.
Silverio, Adolph Christian O.

Adviser:
Engr. John Carlo V. Puno

March 2019

ACKNOWLEDGMENT

The researchers would like to express their deepest gratitude to Dr. Alex Gungab, Ophthalmologist of UST Hospital for sharing his optical expertise and cooperating in this project. To Hon. Luciana Nolasco, Paso De Blas Barangay Captain and the Barangay Officers for giving positive feedback and allowing the proponents to deploy the prototype. To the members of the technical panel, Engr. Nilo Arago, Engr. Aaron Aquino and Engr. Timothy Amado for giving recommendations and encouragements. To the family and friends of the proponents for the financial and emotional support. And above all, to our Almighty God, for providing us hope, knowledge and glory.

ABSTRACT

Over the past years, wavefront technology is used in astronomy because it has better telescopic resolution for examining the universe. Since earth turbulence causes atmospheric aberrations, this technology is the solution compensating it. Human eye also has aberrations, which is divided into two, higher and lower order aberration. In this study, human eye is examined using the wavefront technology to measure the lower order aberration. Refractive errors, or aberrations include myopia (nearsightedness), hyperopia (farsightedness), and astigmatism. When these are left uncorrected, it may lead to severe vision impairment and blindness. In this study, a portable eye checkup device is developed using wavefront aberrometry to measure the refractive errors of the eyes. The device is composed of a wavefront sensor and microcontroller, assembled in a 3D printed case. It also has a touchscreen display which provides a user-friendly interface. The wavefront sensor, which is based on the Shack-Hartmann principle, captures the wavefront of light reflected by the eye. This sensor provides the raw image that will be processed. The Fast Fourier Transform (FFT) of the image is computed and the magnitude and phase spectrum from two peaks surrounding the DC frequency are generated. These values are correlated and computations using formula for Zernike polynomials are performed. The outputs are spherical (SPH), cylindrical (CYL), and axial (AX) values which represent the refractive errors of the eyes. The results are displayed in the device and uploaded to a database which can be viewed at the website online. The device provides reliable measurements which can aid in conducting eye checkups. With this, refractive errors may be detected and corrected at an early stage to prevent severe vision impairments

TABLE OF CONTENTS

Title Page.....	i
Approval Sheet.....	ii
Acknowledgement.....	iii
Abstract.....	iv
Table of Contents.....	v
List of Figures.....	ix
List of Tables.....	xi
List of Equations.....	xii

Chapter 1 The Problem and its Background

1.1	Introduction.....	1
1.2	Background of the Study.....	2
1.3	Statement of the Problem.....	4
1.4	Objectives.....	4
1.5	Significance of the Study.....	5
1.6	Scope and Delimitation.....	5
1.7	Definition of Terms.....	6

Chapter 2 Review of Related Literature

2.1	Conceptual Literature.....	7
2.1.1	Shack-Hartmann Wavefront Sensor.....	7
2.1.1.1	Visual Stimulus.....	8
2.1.1.2	Collimating Lens.....	9
2.1.1.3	Microlens Array.....	9
2.1.1.4	CCD Camera.....	10
2.1.2	Generation of Wavefront Map.....	11
2.1.2.1	Raw Image.....	12
2.1.2.2	Zernike Polynomials.....	12
2.1.2.3	Wavefront Map.....	13
2.1.2.4	Lower-Order Aberrations.....	14
2.1.2.5	Fourier Transform.....	15
2.2	Related Literature.....	15
2.2.1	Foreign Studies.....	15
2.2.2	Local Studies.....	18

Chapter 3 Methodology

3.1	Research Design.....	21
3.1.1	Hardware Construction.....	22
3.1.2	Software Development.....	25
3.2	Materials and Equipment.....	29
3.3	Testing Procedure.....	29
3.4	Evaluation Procedure.....	30
3.5	Data Analysis.....	31
3.6	Gantt Chart.....	33

Chapter 4 Results and Discussion

4.1	Project Technical Description.....	35
4.2	Project Structural Organization.....	36
4.2.1	Device.....	36
4.2.2	Sample Raw Image.....	38
4.2.3	Graphical User Interface.....	39
4.2.4	Website.....	41
4.3	Project Limitation and Capabilities.....	44

4.4	Project Evaluation.....	44
Chapter 5 Summary of Findings, Conclusion and Recommendations		
5.1	Summary of Findings.....	50
5.2	Conclusion.....	50
5.3	Recommendations.....	51
References.....		52
APPENDIX A Needs Assessment.....		60
APPENDIX B Program Codes.....		66
APPENDIX C Bill of Materials.....		83
APPENDIX D Specifications and Datasheets.....		85
APPENDIX E Data Gathered.....		101
APPENDIX F Project Manual.....		105
APPENDIX G Letters and Certifications.....		108
APPENDIX H Project Documentation.....		112
APPENDIX I Researcher's Profile.....		125

LIST OF FIGURES

Figure 1	Collimating Lens
Figure 2	Microlens Array
Figure 3	Raspberry pi Camera Module
Figure 4	Example of Raw Image
Figure 5	Example of Wavefront Map
Figure 6	IPO of the Project
Figure 7	Wavefront Sensor Diagram
Figure 8	Construction of Wavefront Sensor
Figure 9	General block diagram for software development
Figure 10	Development of Graphical-User Interface
Figure 11	Development of Website
Figure 12	Block Diagram of Testing
Figure 13	Block Diagram of Evaluation
Figure 14	Example of Confusion Matrix
Figure 15	Proper position when using the device
Figure 16	SOLLA Eye Check Device
Figure 17	Sample Raw Image
Figure 18	Graphical User Interface
Figure 19	Website
Figure 20	Prototype evaluation

Figure 21	Result obtained from the device
Figure 22	Result obtained from the autorefractometer
Figure 23	Confusion Matrix
Figure 24	Survey Results

LIST OF TABLES

Table 1	Zernike Polynomials in Polar Coordinate
Table 2	Analysis of spherical values
Table 3	Analysis of cylindrical values
Table 4	Analysis of axial values

LIST OF EQUATIONS

Equation 1	Accuracy Rate
Equation 2	Misclassification Rate
Equation 3	Miss Rate
Equation 4	Fall-out Rate

CHAPTER 1

THE PROBLEM AND ITS BACKGROUND

This chapter presents the background of the study, statement of the problem, objectives, significance, and the scope and delimitation of the study.

1.1 Introduction

According to the Department of Health (DOH), approximately 2,511,883 people in the Philippines have vision impairment as of 2017. About 13.22% (332,150) of this population are bilaterally blind, and 25% (83,037) of these cases are due to refractive errors. On the other hand, 86.78% (2,179,733) of this population have low vision impairment, and 43% (937,285) of these cases are due to refractive errors. Moreover, the World Health Organization (WHO) said that about 285 million people in the world have vision impairments. About 86% of this population are with low vision impairments and the remaining 14% of this population are blind. These statistics show that majority of the population has low vision impairments, and these are commonly caused by refractive errors.

Vision impairments are imperfections of the human eyes that prevent light from focusing properly on the retina, which impairs the quality of the visual image. These are also called wavefront aberrations which can be categorized into two kinds, the lower order aberrations (LOA) and the higher order aberrations (HOA). LOA, which comprises the 0, 1st, and 2nd order aberrations, define the refractive errors in the eyes which are usually corrected by eyeglasses, contact lenses, or refractive surgery. HOA, which comprises the

3rd to nth order aberrations, define optical imperfections such as coma, trefoil, etc. which are often hard to correct with the present technology.

The refractive errors or LOA can be categorized into three types, namely, myopia, hyperopia, and astigmatism. Myopia or nearsightedness occurs when light rays focus before the retina, producing a blurred vision for far objects. Hyperopia or farsightedness occurs when light rays focus behind the retina, producing a blurred vision for nearby objects. Astigmatism, on the other hand, occurs when the cornea of the eye is irregularly shaped, causing objects at any distance to be out of focus. Although these refractive errors in the eyes can be corrected by eyeglasses, contact lenses, or refractive surgeries, it may lead to worse cases or even blindness, if not treated immediately.

There are a variety of reasons why most refractive errors are left uncorrected. This includes the lack of awareness regarding the proper eye care and the limited services offered for eye checkups. Up to date, eye clinics in the country use autorefractometers which follows refraction assessment using low vision eye charts and phoropters. The low vision eye charts use a subjective method for prescriptions, and all the autorefractometers being used in the country are imported and costs more than half a million pesos. Moreover, the latest statistics says that the ratio of the ophthalmologists in practice and in training to the population in the Philippines is 14: 1,000,000. This means that there are only around 1,400 ophthalmologists in the country.

1.2 Background of the Study

Several technology advancements have been made towards the measurement of refractive errors in the eyes. The early methods used, which are still used in every eye

checkup conducted up to date, are subjective eye examinations. These eye checkups require the feedback of the patient to acquire an accurate result. Typically, optometrists and ophthalmologist utilize the use of specialized low vision eye charts. After asking the patient to read out lines from the chart, the next process will be the refraction assessment. Nowadays, the most common eye checkup device found in eye clinics is the autorefractometer. The autorefractometer estimates the refractive errors in the eyes.

One of the new technologies used in measuring the refractive errors in the eyes is the wavefront aberrometry. Wavefront technology or aberrometry describes the way light rays travel through the eyes. The wavefront technology can diagnose both the lower and higher order aberrations in the eyes objectively.

Based on the statistics, about 40.61% (1,020,323) of the people who are suffering from vision impairments are due to refractive errors. When these refractive errors are left uncorrected, they may cause severe visual impairment and may even lead to blindness. Detecting these optical impairments at an early stage and providing accessible eye care services can help keep the eyes in a good condition and avoid these common causes of blindness.

This study will address the problem of the limited availability of the eye checkup services in the Philippines which is one of the main reasons why there are uncorrected refractive errors. Using the latest technology, wavefront technology, eye checkups in the country will be more efficient and provide a more accurate result as this eye examination is not subjective.

1.3 Statement of the Problem

This study, Measurement of Lower-Order Aberrations in the Eyes Using Wavefront Aberrometry based on a CCD Camera, seeks to find answers to the following questions:

- How will an eye checkup equipment be constructed so that it will provide accurate measurements of refractive errors in the eye?
- What components and/or devices shall be used so that it can be portable and be easily accessed?
- How will the people's awareness about the significance of regular eye checkups be raised?

1.4 Objectives

This study generally aims to construct a portable eye checkup device that will measure the refractive error (myopia, hyperopia, and astigmatism) present in the eyes accurately. The following are the specific objectives of the study:

1. To design a Shack-Hartmann wavefront sensor that will provide a quality raw data
2. To develop a program using Python that will reconstruct and process the captured image to generate a wavefront map
3. To develop a user-friendly graphical user interface (GUI) that will display the results of the eye checkup
4. To compare the results of the study with the commercially available aberrometers to measure its accuracy
5. To provide a portable aberrometer that will aid the ophthalmologists/optometrists in measuring the refractive error

1.5 Significance of the Study

Raising the awareness of individuals and the availability and quality of eye checkups in every community is very important. The early detection of the refractive errors in the eyes and the immediate correction using contact lenses, eyeglasses, or refractive surgeries will prevent further complications that may occur. These refractive errors, when not addressed or left uncorrected, may even lead to blindness.

Also, having a locally made portable eye examination device which uses the latest technology is a huge advancement in the field of optometry and ophthalmology in the Philippines. It will be a great help for the practitioners as the wavefront aberrometer gives accurate results and portable which means it can be easily deployed to many different places.

1.6 Scope and Delimitation

The focus of this study is to construct a portable eye checkup device that will measure the refractive errors in the eyes accurately. This study will confine itself to the measurement of the lower order aberrations (LOA), which include myopia, hyperopia, and astigmatism. This study will also use the Shack-Hartmann principle for the construction of the wavefront sensor. It will also use Zernike polynomials and Fast Fourier Transform (FFT) for the algorithm in generating the wavefront map.

This study will exclude the identification of the higher order aberrations (HOA) that may or may not be present in the eyes.

The project can be used by all eye practitioners, optometrists, and ophthalmologists to aid in the measurement of refractive errors. Their needs and preferences were taken into consideration for the design and construction of the eye checkup device.

1.7 Definition of Terms

- Wavefront – a surface over which an optical wave has a constant phase; measured, processed, and reconstructed to generate a wavefront map
- Shack-Hartmann wavefront sensor – measures wavefront aberrations by letting the light impinge on a screen with an array of pinhole openings
- Zernike Polynomials – algorithm that will be used to interpret optical test results
- Fast-Fourier Transform (FFT) – algorithm that will be used in analyzing the raw image and providing the aberration map
- Spherical Power (SPH) – describes the amount of lens power needed to correct myopia or hyperopia; parameter to be used for measurement of refractive errors
- Cylindrical Power (CYL) – describes the strength of astigmatism; parameter to be used for measurement of refractive errors
- Cylindrical Axis (AXIS) – describes the orientation of astigmatism; parameter to be used for measurement of refractive errors

CHAPTER 2

REVIEW OF RELATED LITERATURE

This chapter includes the background theories, principles, and studies useful in the development of the idea in conceptualizing of the project. This include technical terminologies used from the past and present project developed.

2.1 Conceptual Literature

2.1.1 Shack-Hartmann Wavefront Sensor

Shack Hartmann wavefront sensors can be used for various applications. However, these wavefront sensors need to be assembled. They have a specific setup along with other devices for a specific application. When the light passes through the eye, it reflects and creates a wavefront. When this wavefront enters the lenslet array, the array will split it into discrete sections, one section for every lenslet. Assume that the lenslet to be small compared to the curvature of the wavefront, the wavefront can be assumed to be flat over each lenslet. Therefore, each lenslet will focus its part of the incoming wavefront to a spot on the CCD. In an eye without aberrations, the wavefront creates a perfect grid, while an eye with aberrations will yield a distorted grid on the CCD Camera. The spots diverge in horizontal and vertical manner from the optical axis of the lenslet.

2.1.1.1 Visual Stimulus

The visual stimulus that is commonly used is a near infrared laser diode. A portion of the light from the stimulus reflects and is re-emitted out from the eye as if it came from a specific source point on the retina. The wavefront that exits the eye, enters the microlens array which divides it into several small light rays. It is important to choose a safe light source, considering three factors. Primarily, it must be safe for the human eyes. The safest color that can be used is red for it has longer wavelength and narrow.

It is important to choose for the safest light source to be used. When choosing the light source for the Shack-Hartmann Wavefront sensor, there are three factors must be considered. Primarily, the light should be safe for the human eyes. The safest color to use is red for it has the longest wavelength but narrow bandwidth. Second, the light must be collimated (parallel) when emitted, or easy to collimate. Lastly, it must be intense enough to ensure that a enough intensity reaches the CCD, or the Shack-Hartmann Wavefront sensor pattern of spots will faint resulting to error.

For the light source, it was recommended by the Ophthalmologist to use either Fiber-Optic Laser Diode or Light-Emitting Diode (LED). Fiber-Optic Laser Diode, which most easily could be described as a laser diode where the light only passes once through the cavity. The light is monochromatic, and the coherence is low.

2.1.1.2 Collimating Lens

The light rays coming out from the light source spreads divergently so as the need of a collimating lens to convert these rays into a parallel beam of light. It was designed, not just to convert the beam, but to act as a support in achieving a certain spatial resolution setup and to reduce the divergence angle.



Figure 1 Collimating Lens

2.1.1.3 Microlens Array

The sensitivity of the Shack-Hartmann Wavefront sensor improves proportionally to the focal length of the microlens array. Microlens array is a small lens, with a diameter less than a millimeter (mm) and often as small as 10 micrometers (μm). It is fabricated in glass and fused silica and coated with patterned aluminum or chromium. Microlens arrays are efficient in terms of gathering light and providing smaller and brighter spots which is useful for lowlight applications. The wavefront that exits the eyes and enters through the microlens array and then brakes into discrete small light rays.

The local slope of the wavefront that exits the lenslet array provides the position of the spot in the raw image. The wavefront aberration is produced by the mathematical integration of information across all the spots from the lenslet array.

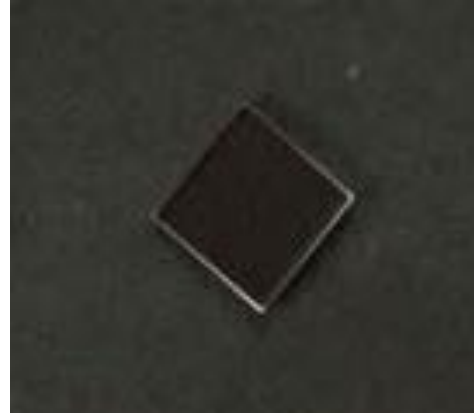


Figure 2 Microlens Array

2.1.1.4 CCD Camera

The spatial resolution achievable in the Shack-Hartmann sensor depends on the camera in use. CCD camera is the best photodetector to be used, it converts light to electrical charges and create high quality, low noise images. The wavefront to be reconstructed is sampled by a screen with many lenslet. Each lenslet produces a light spot on the screen or position sensitive high-resolution CCD camera. The Raspberry Pi Camera is an image sensor custom designed add-on board for Raspberry Pi, that has feature where in lens can be focused. This feature can be used to capture the image of the eyes. The captured image is transferred to the software where it is processed and analyzed.

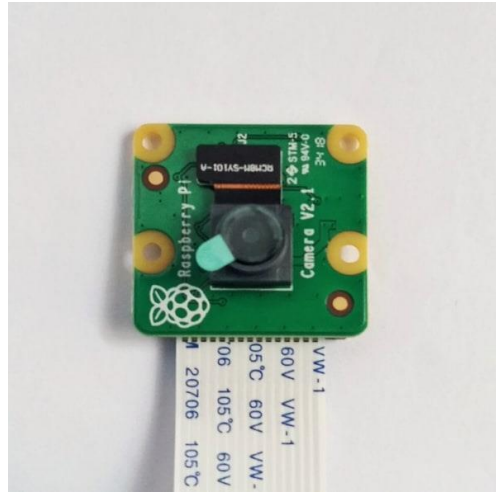


Figure 3 Raspberry pi Camera module

2.1.2 Generation of Wavefront Map

The wavefront map provides a complete and accurate information that is helpful in detecting all aberrations affecting the eye. The doctor uses wavefront map as a blueprint for providing the accurate vision correction treatment. Wavefront map gives specific data regarding aberrations expressed in microns of deviation from an ideal planar wavefront. The output contains both two- and three-dimensional map that contains total aberration. The defocus (myopia and hyperopia) and astigmatism can also be seen through the wavefront map.

2.1.2.1 Raw Image

It is captured by the Shack-Hartmann wavefront sensor which comprises the CCD camera and the microlens array. This is the baseline of the output. A Shack-Hartmann sensor's measurement accuracy depends on

its ability to precisely measure the displacement of a focused spot with respect to a reference position.

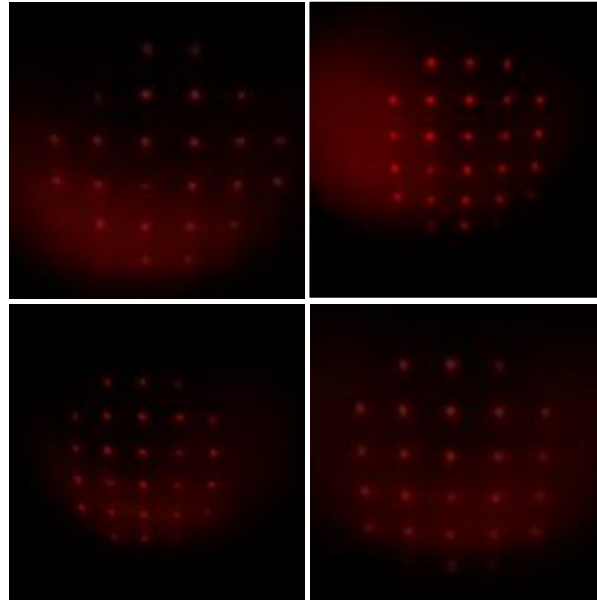


Figure 4 Example of Raw Image

2.1.2.2 Zernike Polynomials

Optical system aberrations have historically been characterized by power series expansions, where the wave aberration is expressed as a weighted sum of power series terms that are functions of the pupil coordinates. Each term is associated with a particular mode. There are numerous optical systems that have circular pupils. There are also various analyses and calculations (e.g. diffraction) that involve the integration of the pupil function and wave aberration function over a circular pupil. Experimental measurements will also be performed over a circular pupil and will commonly require some form of data fitting. It is, therefore,

convenient to expand the wave aberration in terms of a complete set of bases of functions that are orthogonal over the interior of a circle.

Zernike polynomials are commonly used in the analysis of adaptive optics systems and are also used to interpret optical test results. They form a complete set of functions or modes that are orthogonal over a unit circle and are convenient for serving as the set of bases of the function. They are usually expressed in polar coordinates and are readily convertible to Cartesian coordinates.

2.1.2.3 Wavefront Map

The wavefront map of an eye indicates the distance between the reflected wavefront and the pupil plane which represents an error of optical path length which varies from point-to-point across the pupil. The aberration map can be quantified by a mathematical function W (can be obtained using Zernike Polynomials) that depends on the x- and y-coordinates of points inside the eye's pupil. Each point in the pupil plane can be located by its x- and y- coordinates or in terms of the polar coordinates, r and θ . Thus, the aberration map can be understood and displayed using all 3 formats of ray optics, optical path errors, and wavefront shape errors regardless of whether the light is propagating into the eye or reflected out of the eye. Moreover, the Zernike coefficients obtained from the map, provided that the modes specifically are 3, 4, and 5, representing the LOA, can be used to obtain the parameters needed for interpretation of clinical results.

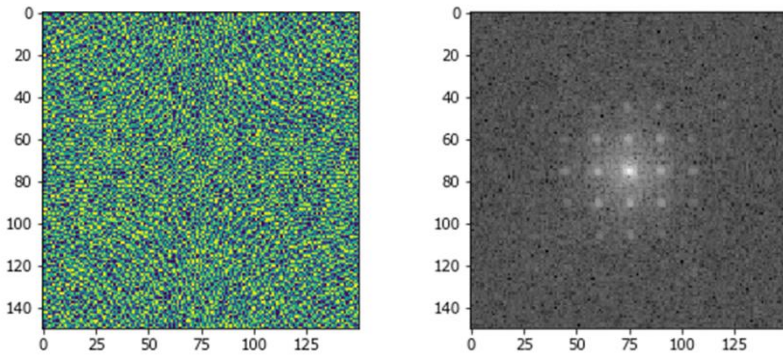


Figure 5 Example of Wavefront Map

2.1.2.4 Lower-Order Aberrations

Lower-order aberrations (LOA) are the defocus (myopia and hyperopia) and astigmatism. Myopia occurs due to an irregularly shaped cornea which causes light rays to focus in front of the retina, rather than directly on the retina, while hyperopia light is focused behind the retina, rather than directly on the retina and astigmatism is when the eye is shaped like oval. The lower order aberrations may be acquired from the wavefront map.

2.1.2.5 Fourier Transform

Fourier transform is one of the most important image processing tools used to decompose an image into its sine and cosine components. The input image is in spatial domain equivalent while the output of the transformation represents the image in Fourier domain. In the Fourier domain image, each point represents a particular frequency contained in the special domain image. One spot in Fourier space contains information about

all the spots from the CCD space. In Fourier space, only two spots are needed to be analyzed to get the SPH, CYL, and AXIS. The noise is pushed to the edge of the Fourier image, since it tends to have much higher than the spot pattern. The central peaks of the image are very “clean” since the modulus of the Fourier transform is independent of decentration of the pupil.

2.2 Related Literature

2.2.1 Foreign Studies

In the study “A simple and effective algorithm for detection of arbitrary Hartmann-Shack patterns,” the researchers developed an algorithm for detecting Shack-Hartmann patterns by using a commercially available hardware and easy to use software. The Shack-Hartmann sensor is popular in detecting wavefront deviations from telescopic images.

The results obtained were accepted in clinical measurements, since, the expected results were met. The deviations compared to the simulated values were 0.2 D for sphere, 0.1 D for cylinder, and 0° for axis. They believed that this algorithm will be helpful in the development of the next generations autorefractors.

In the study entitled “Total Aberrations Measurement with Using the Mathematical Model of the Eye” by Fatemeh Devarinia and Zahra Akhyani, Keyban Maghooli from Islamic Azad University, by using the Ray tracing method, the researchers simulated the Shack-Hartmann principle, and were able to extract

dioptric power from the corneal topography images. The shape of the wavefront exiting from the eye was reconstructed using Zernike Polynomials. Three parameters were calculated, the Sphere, Cylinder, and Axis parameters that are used as guide for the correcting glasses. The Zernike coefficients were determined by fitting the measured tilts to the derivatives of the Zernike polynomials.

A study entitled “Human Eye Aberration Measurement and Correction Based on Micro Adaptive Optics System,” characterized Shack-Hartmann wavefront sensor as the most well-known adaptive optics system because it has a wide scope of applications in the field of optics.

Using the least square method, there will be residual coefficients in the wavefront removal of aberrations. In the study “A New Method for Improving the Accuracy of Wavefront Fitting Zernike Polynomials,” the researchers described a modified method to perform more accurate Zernike coefficients with respect to the wavefront. Zernike polynomials are used in representations in many different fields of optics. In order to know the exact aberrations, the Zernike coefficients must be known. The new method divided the form of wavefront fitting into two parts. The orthogonal polynomial coefficients are obtained using least square method for the both parts.

Through their calculations, the results showed that the method that the using least square method, there are obvious deviations between the fitting results and the simulated coefficients. While the modified method by the researcher gave better results either in coefficients or in standard deviation.

A study entitled “Zernike and Fourier Wavefront Reconstruction Algorithms in Representing Corneal Aberration of Normal and Abnormal Eyes” tested the accuracy of Zernike and Fourier reconstruction algorithms in describing wavefront simulations from corneal topography of normal and abnormal eyes. They collected corneal topography on normal and with different eye defects. The original data from the slit images were converted into elevations and the resampled to different resolution they need in testing. The conventional Zernike and iterative Fourier algorithms were both used to reconstruct the elevation map that was obtained from the raw data from slit images. To evaluate the reconstruction performance, the researchers used the residual RMS error to quantify difference between the reconstructed and the original maps.

The study showed that with the Zernike-based method, the remaining RMS errors lessened as the number of modes increased. With this method, the reconstructions of the wavefront maps of low spatial resolution were inaccurate when used with large number of Zernike modes while the Fourier algorithm had more reliable reconstructions in the center of the pupil than peripherally. It is concluded that the Zernike method is better than the Fourier method when used in representation of wavefront data simulations from topography maps.

In an article entitled “A Comparison of a Traditional and Wavefront Autorefraction,” the researchers compared the autorefraction obtained using a wavefront sensor and a conventional ray deflecting principle device. They used a 0.25D clinically significant variance between spherical and cross-cylinder measurements because results from phoropters and clinical eye tests vary by a

minimum of 0.25D. The results showed that the conventional autorefractor was slightly more accurate for measuring cylindrical power than a subjective refraction.

According to the study “Wavefront Sensors for Adaptive Optical,” Shack-Hartmann sensor is widely used in atmospheric applications. This device was developed using a laser light as a light source and it can be used in different applications for the field of adaptive optics. The developed software for the wavefront sensor has a capability to select which algorithm is to be used depending on the applications, which are modified centroids, normalized cross-correlation and fast Fourier demodulation used in wavefront slope elimination. It also includes methods for the wavefront reconstruction which are modal Zernike polynomial expansion, deformable mirror response function expansion and phase unwrapping. This increases the range of the Shack-Hartmann sensor application.

2.2.2 Local Studies

An article published by Manila Bulletin, reported that by 2016, there are about 300,000 number of Filipinos who are suffering from blindness according to Department of Health. There are 295,152 Filipinos with both eyes blind, out of these, 59 percent were because of cataract and 14 percent are because of uncorrected refractive errors.

According to an article from Philippine Journal of Ophthalmology, myopia is the leading type of refractive error. In the study there are 666 patients who took optical biometry measurements. It was concluded that based on age, elderly people

were categorized with shorter axial length and dominant hyperopia while based on the gender, it showed that there are no significant differences.

One article stated that the older age groups are more likely to have a shorter axial length and hyperopic than the younger population, which were more myopic. It is stated in the article that corneal curvature flattens with age which results to prevalent hyperopia in the older people.

An original article from Philippine Journal of Ophthalmology compared the efficacy, safety, refractive and visual outcomes, and aberrometry results of wavefront-guided aspheric treatment (WTA) versus wavefront-guided treatment. LASER-IN-SITU keratomileusis (LASIK) is a widely accepted and used procedure for correcting refractive errors. There are 60 eyes of 30 patients who underwent myopic LASIK included in this study where one eye of each patient was randomized to either wavefront-guided aspheric treatment or wavefront-guided. Patients were followed up for 3 months postoperatively

To determine statistical significance the researchers used two-tailed paired t-test. The study concluded that wavefront aspheric LASIK (WTA) is a safe and effective treatment for myopic astigmatism. While the WTA had less induction of higher-order aberration, lower spherical aberration, and better preservation of corneal a sphericity (Q value). The refractive and visual outcomes were similar for both groups.

A study from The International Eye Institute of St. Luke's Medical Center, stated that according to the World Health Organization about 314 million people in

the world suffer from low vision impairments and blindness. According to them the leading cause of blindness is cataract and uncorrected refractive error causes visual impairment. The WHO stated that by 2020, global blindness might reach 76 million. Some factors that affect eye vision are “age (50 years and above), female gender, socioeconomic status in developing countries, exposure to UV radiation, vitamin A deficiency, high body mass index, and metabolic disorders.”

CHAPTER 3

METHODOLOGY

This chapter contains the block diagram in construction the wavefront aberrometer, and the algorithm for development of the program, GUI and website.

3.1 Research Design

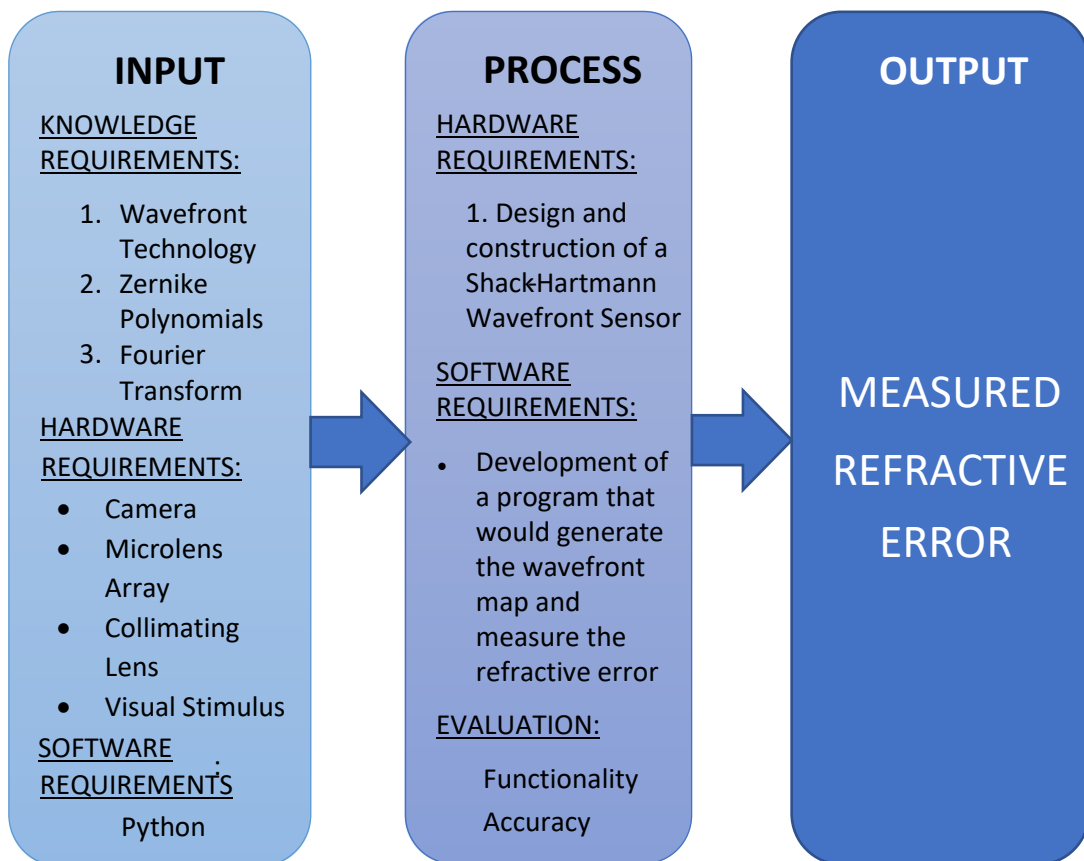


Figure 6. IPO of the project

In this project, the general objective is to develop a wavefront aberrometer that would accurately measure the refractive error of human eye. Knowledge about wavefront technology, Zernike polynomials and Fourier transform are needed. Camera, microlens array, collimating lens and visual stimulus are the main components of the device that will be constructed. After capturing the raw data, the image will undergo processing to generate the wavefront map. Relevant data will be extracted from the generated map to obtain the refractive error.

3.1.1 Hardware Construction

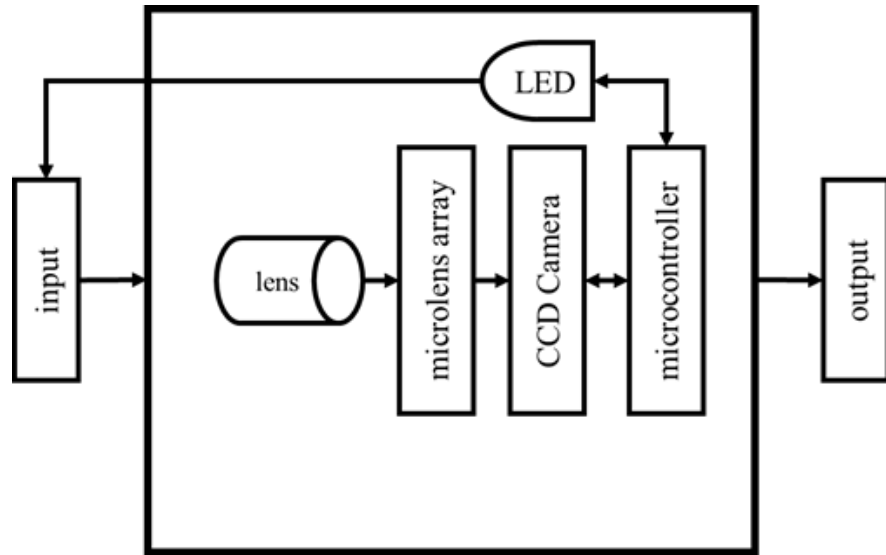
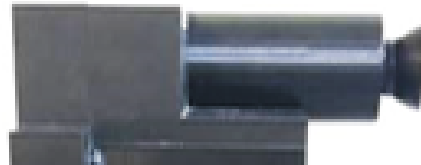


Figure 7. Wavefront Sensor Diagram

As the light from the visual stimulus enters the human eye, it is reflected and produces a wavefront. The visual stimulus that is used in this sensor is a red Light-Emitting Diode (LED) that has a wavelength under the group, Retinal thermal-weak visual stimulus. The LED is controlled by the microcontroller. The microlens array will divide the incoming wavefront into discrete sections, one

section is allotted each lenslet. Therefore, the incoming wavefront will be focused by each lenslet to a spot in the CCD Camera. In an eye without aberrations, the wavefront creates a perfect grid, while an eye with aberrations will yield a distorted grid on the CCD Camera. The spots diverge in horizontal and vertical manner from the optical axis of the lenslet. [25] [26] For collection efficiency and spatial resolution of the setup, using collimating lens will be suitable. The CCD Camera, which is also connected to the microcontroller, will capture the wavefront in 5 seconds. This output produces the raw image that will be processed by the program depending which aberration is needed to be detected.



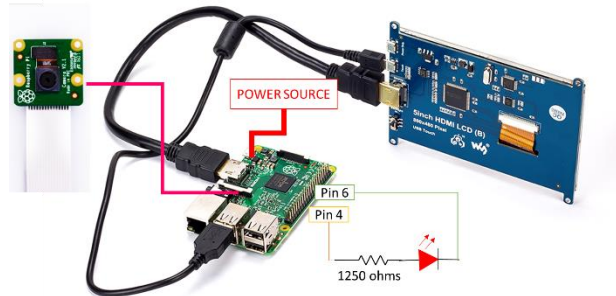
(a)



(b)



(c)



(d)

Figure 8. Construction of Wavefront Sensors (a) top (b) components inside the monocular (c) base (d) wiring inside the base

In figure 8.a shows the top part of the prototype, it is designed like a telescope. It has an eyecup where the users can peek for them to be examined. While in Figure 8.b shows what's inside the monocular, it is composed of the camera and its ribbon, which is connected to the microcontroller, the collimating lens and microlens array. The base which is 3D Printed, as shown in Figure 8.c. The prototype is composed of the screen where the program and results can be seen, power bank as the power source, circuit for the LED, switch for turning on and off

the prototype and the microcontroller. The wiring and configuration of the raspberry pi to the pi camera and screen is shown in Figure 8.d.

3.1.2 Software Development

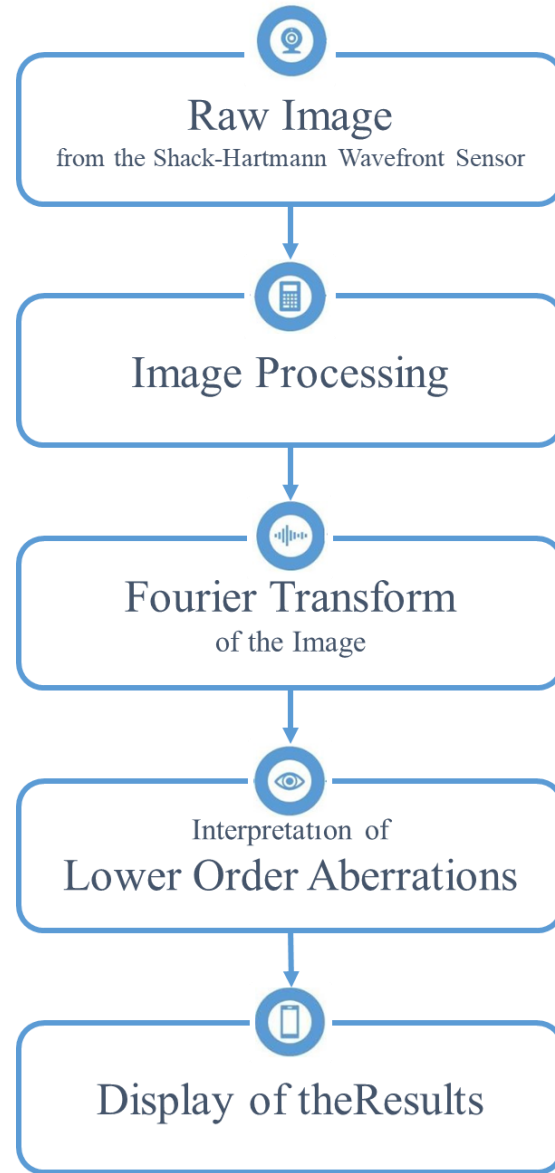


Figure 9. General block diagram for software development

Python, an open source programming language which can utilize advanced programming. It can analyze mathematical models and perform calculations and applications, for instance signal processing. The program developed using Python will process the incoming raw image from the Shack-Hartmann wavefront sensor instantly as soon as the sensor captures the image. This raw image is processed to reduce the noise. Gaussian filtering smoothens the image and is highly effective in eliminating Gaussian noise. The median filter is also applied to further improve the image. After these processes, the filtered image is reconstructed using the fast Fourier transform. This moves the DC frequency to the center.

The magnitude and phase spectrum of the transformed image is generated and two peak values surrounding the central frequency are obtained. These values are correlated and used for the aberration metric, with the magnitude as rho (ρ) and the phase as theta (θ). The correlations of these two values will be used in some mathematical computations using Zernike polynomials. From these, the values of the refractive errors of the eyes are obtained. These are the spherical (SPH), cylindrical (CYL) and axial (AX) values, respectively.

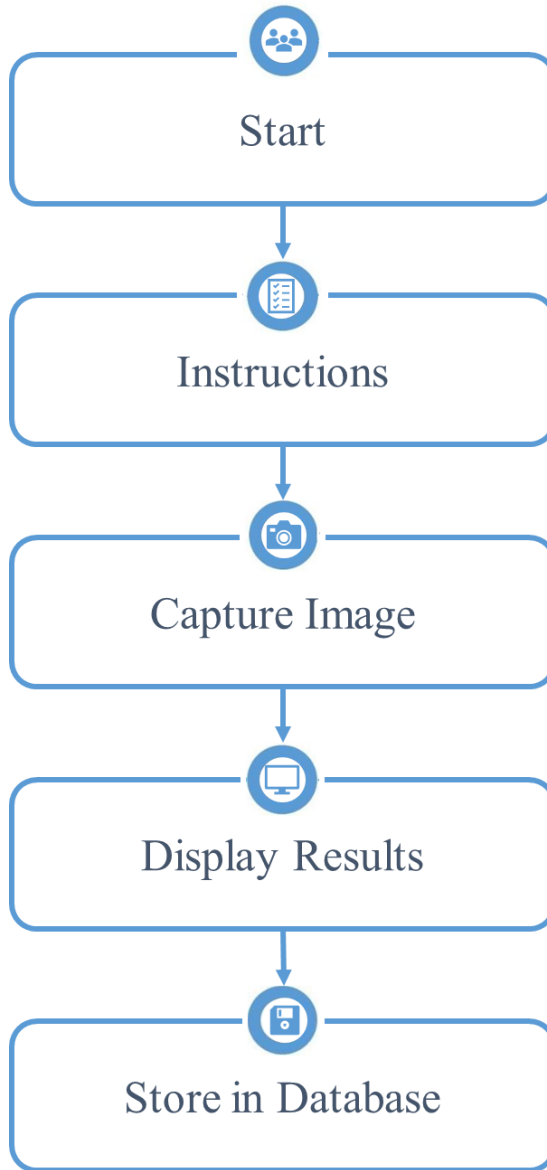


Figure 10. Development of Graphical-User Interface

The user interface was developed using guizero, a Python 3 library used in creating GUIs. The GUI displayed the instructions that will guide the user on how to use the device. There are buttons used for capturing the image from the left and right eye and the GUI also showed the image captured. The results obtained from

the both eyes which are spherical, cylindrical and axial were displayed in the GUI and stored in the database.

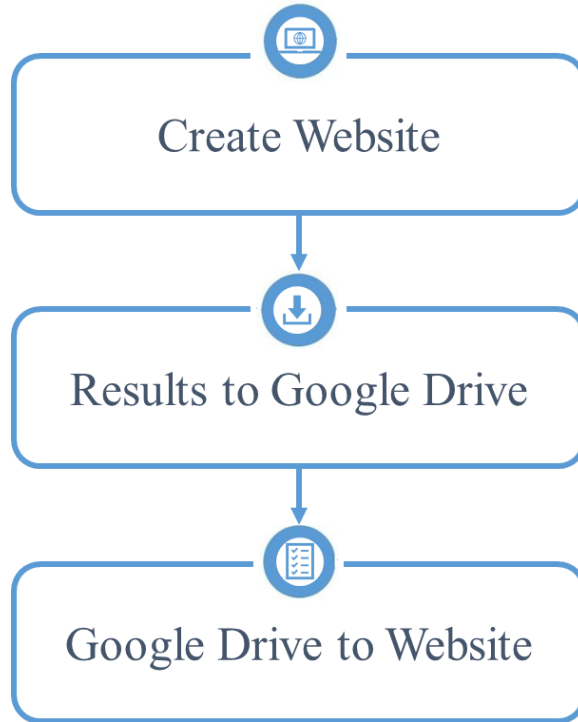


Figure 11. Development of Website

The website is created using WordPress software that is based on PHP and MySQL. The interface is created to be informative and accessible for the users online. The results which are the SPH, CYL and AX obtained from the left and right eye were sent to the google drive using Python. The data on the google drive spreadsheet were published to the web by embedding the HTML to the page. As the spreadsheet updates with the results, the website is automatically updated in real-time also.

3.2 Materials and Equipment

- Visual Stimulus
- Collimating Lens
- Microlens Array
- CCD Camera
- Raspberry Pi

3.3 Testing Procedure

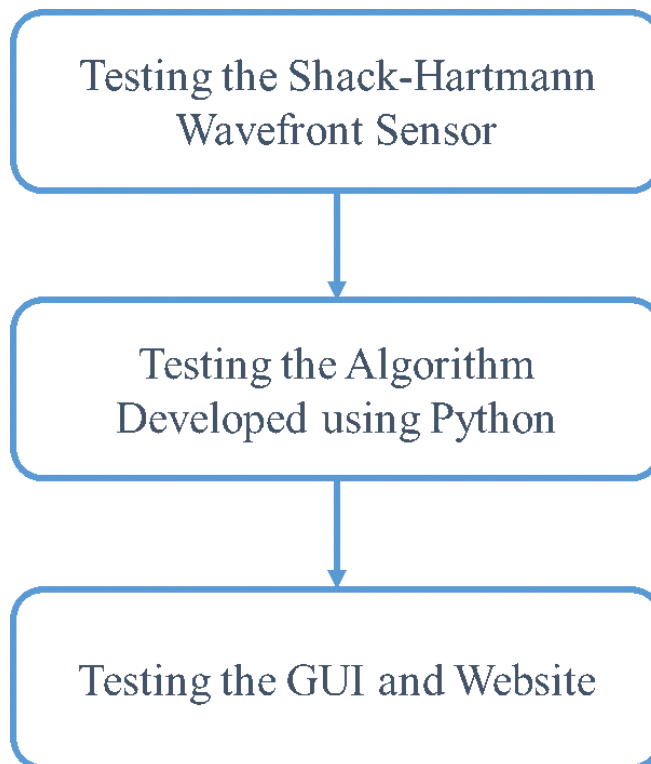


Figure 12. Block Diagram of Testing

In testing the Shack-Hartmann wavefront sensor, a wavefront should be generated and captured from the human eye. The output should be a raw image representing the wavefront reflected by the eyes.

In testing the algorithm developed using Python, the raw image from the Shack-Hartmann wavefront sensor will serve as the input. The program must be able to process the image and extract the necessary data to provide the refractive errors.

In testing the GUI, the user should be able to use the device to capture the eyes when the patient is ready and see the results displayed on the screen. The results should also be uploaded in the website after the whole process is done.

3.4 Evaluation Procedure

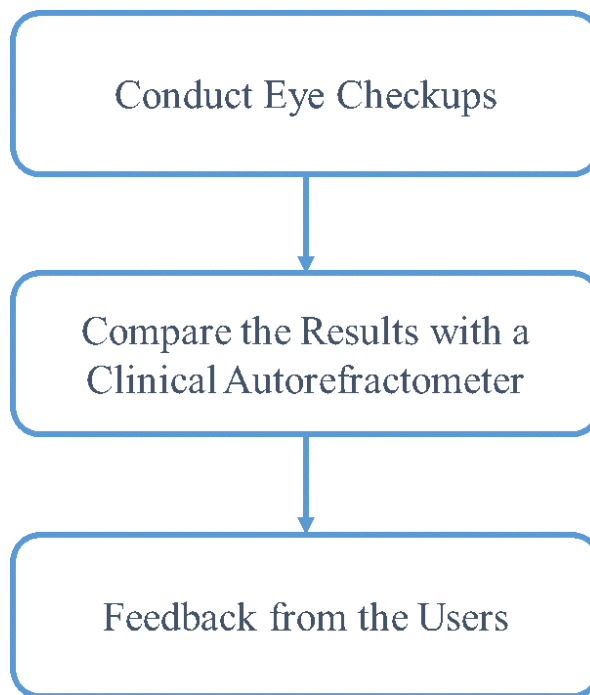


Figure 13. Block Diagram of Evaluation

To evaluate the performance of the device, the researchers will gather data by conducting eye checkups. The results obtained from the eye checkup using the device will be compared with the results from the subject's eye checkup using a clinical autorefractometer. This will assess the accuracy of the device. The subjects will also provide a feedback after using the device in order to assess its performance.

3.5 Data Analysis

The data gathered by conducting eye checkups will be compared with the results obtained by clinical autorefractometers. The spherical, cylindrical, and axial values will be analyzed. The spherical value specifies if the patient have either myopia or hyperopia. Prescriptions with myopia or nearsightedness manifests a negative number while prescriptions with hyperopia or farsightedness manifests a positive number which indicates the amount of refractive error present. The cylindrical value specifies if the patient has some form of astigmatism. The axis indicates the orientation of astigmatism. This number will be between 0 to 180 degrees and can change over time.

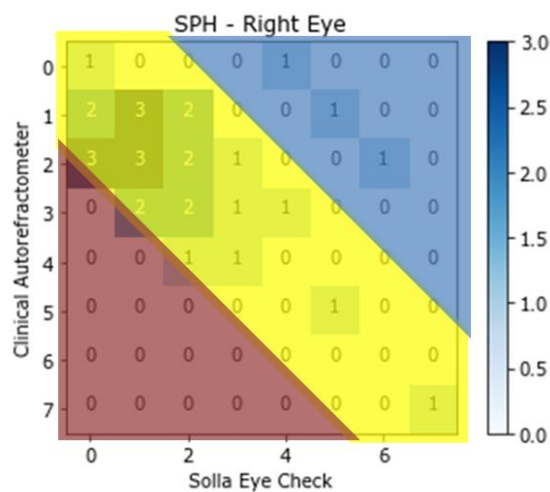


Figure 14. Example of Confusion Matrix

These data will be compared and analyzed by using confusion matrix. The yellow-shaded area of the example of confusion matrix as shown in Figure 14 are equivalent to the true positive and true negative values. The red-shaded and blue-shaded areas represent the false negatives and false positives, respectively. False negatives indicate the times that the device predicts lower values than the actual values while false positives indicate the times that the device predicted higher values than the actual values. There are many measures that can be used to interpret the confusion matrix. In this study, the accuracy, misclassification or error rate, miss rate, and fall-out rate will be used. The formulas for computations are shown in Equations 1-4. The values that will be obtained for the spherical, cylindrical, and axial refractive errors will be averaged to assess the overall performance of the device.

$$Accuracy = \frac{\Sigma True Positive + True Negative}{\Sigma Total Samples}$$

Equation 1. Accuracy rate

$$Misclassification Rate = 1 - Accuracy Rate$$

Equation 2. Misclassification rate

$$Miss Rate = \frac{\Sigma False Negative}{\Sigma Condition Positive}$$

Equation 3. Miss rate

$$Fall-out Rate = \frac{\Sigma False Positive}{\Sigma Condition Negative}$$

Equation 4. Fall-out rate

3.6 Gantt Chart

	Nov	Dec	Jan	Feb	Mar	Apr	May	Jun
Deliberation of Project Ideas								
Intensive Research about the Topics								
Final Selection of Topic								
Preparation for Topic Defense								
Topic Defense								
Preparation for Title Defense								
Acquiring Components								
Title Defense								
Drafting Chapter 1-3								
Revision of Papers								
Submission of Chapter 1-3								
Expected Time of Arrival of Components Ordered								
Construction of Shack-Hartmann Wavefront Sensor								
Calibration of the Shack-Hartmann Wavefront Sensor								

	Jul	Aug	Sep	Oct	Nov	Dec	Jan	Feb	Mar
Progress Defense									
Programming: Generation of Wavefront Map									
Programming: Extraction of Data from the Wavefront Map									
Construction of the Graphical User Interface (GUI)									
Testing of Accuracy of the Device									
Pre-final Defense									
Revisions of the Programs									
Preparation for Deployment									
Deployment									
Evaluation of the Projects: Surveys and Data Gathering									
Drafting Chapter 1-5									
Final Defense									
Revision of Papers									
Submission of the Book									

CHAPTER 4

RESULTS AND DISCUSSION

4.1 Project Technical Description

The purpose of this study was to develop a device that is similar to the traditional autorefractometer but will introduce a different method, convenient and is lesser in terms of cost. The device is expected to give the same results as the traditional autorefractometer with the ease of use. This project used microlens array to collect the wavefront of light that is reflected from the eye, which is very small in size to minimize the size and weigh down the cost of the device without affecting the results.



Figure 15. Proper position when using the device

The user needs to align his/her eyes with the eyecup and make it sure that the red light strikes the eyes. The other eye can be covered by the hands while processing the other half. The tripod can be adjusted depending on the height of the user. The camera will capture the raw image and will be processed to generate the reconstructed Wavefront image. Relevant data will be extracted from the reconstructed wavefront image that provides the most direct visualization of the result of wavefront sensing. From the data, Zernike Coefficients will be obtained which are needed to compute for the axial, cylindrical and spherical aberrations.

4.2 Project Structural Organization

4.2.1 Device



Figure 16.a Solla Eye Check Device



Figure 16.b Right side view of the Device



Figure 16.c Left side view of the Device



Figure 16.d Back View of the Device

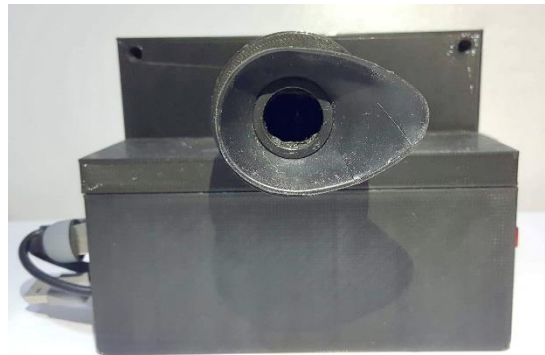
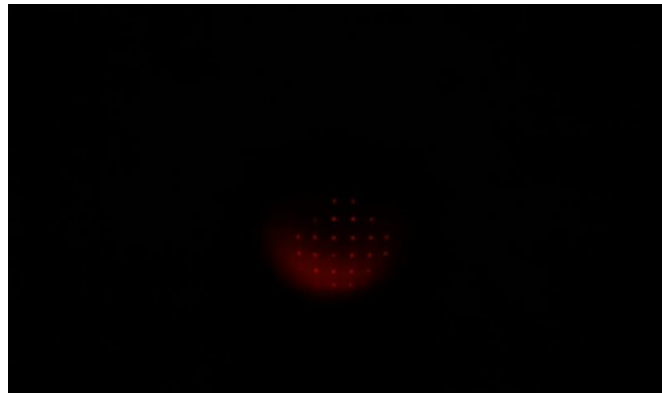


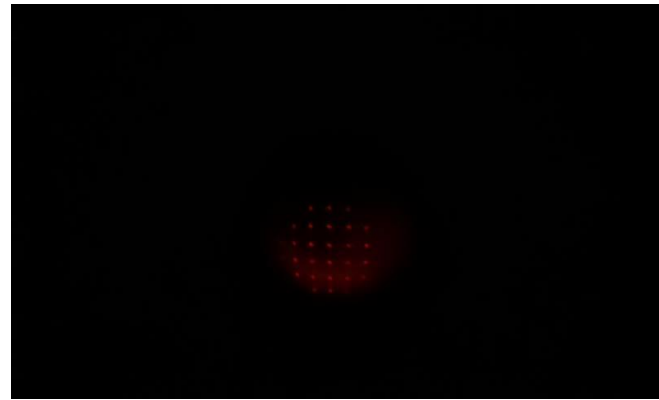
Figure 16.e Front view of the Device

The final structure of the device is shown in Figure 16.a. It has a dimension of (130x280x125mm). In Figure 16.b, the location of the switch is shown. The ports of the device are shown in Figure 16.c, and the LCD display is in Figure 16.d. The side where the patient will peek is shown in Figure 16.e.

4.2.2 Sample Raw Image



(a)



(b)

Figure 17 Raw image from the wavefront sensor (a) left eye (b) right eye

Figure 17 shows the sample raw images that was obtained from the wavefront sensor. This raw image contains spots, wherein each spot contains relevant data and information that is useful for measuring the refractive error. Once processed using different algorithms, data from each image will be very helpful in obtaining the desired output.

4.2.3 Graphical User Interface

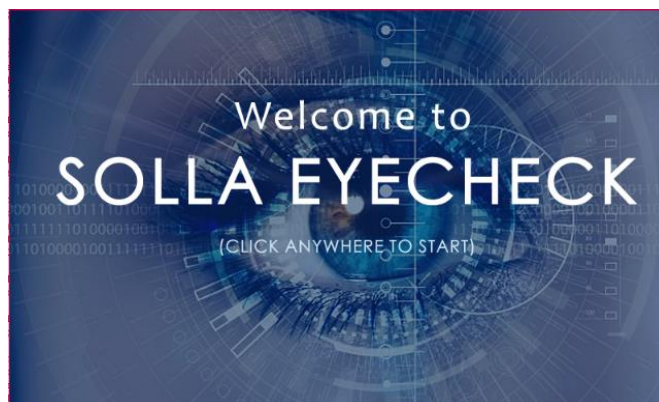


Figure 18.a GUI main window



Figure 18.b Display of instructions



Figure 18.c Capture Button for Left Eye

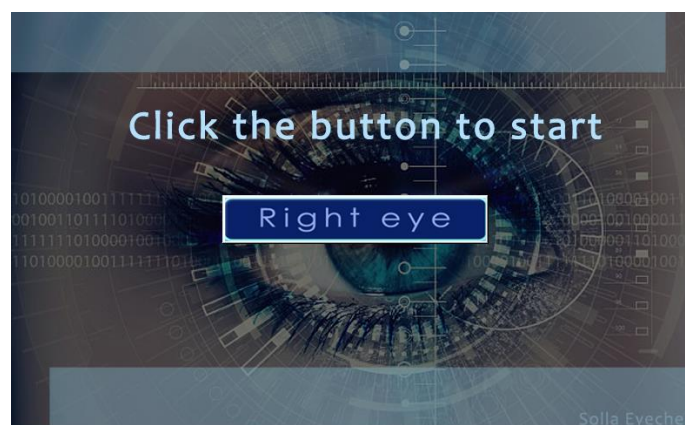


Figure 18.d Capture Button for Right Eye

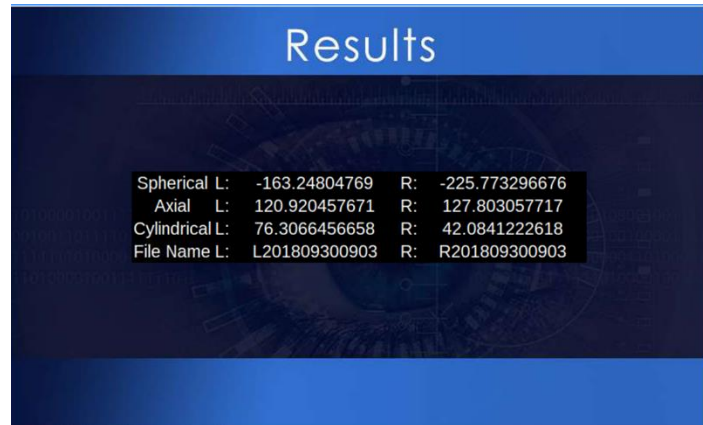


Figure 18.e Results Display

The main window of the user interface is shown in Figure 18.a, while figure 18.b shows the window where the instructions are displayed. The windows for the capture buttons of the left and right eye can be seen in Figures 18.c and 18.d, respectively. The results will be displayed on the window shown in Figure 18.e.

4.2.4 Website

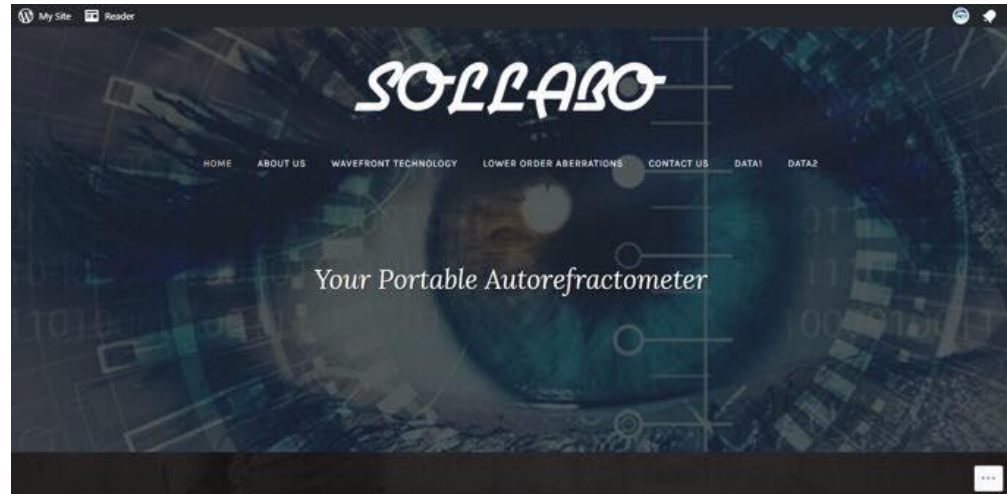


Figure 19.a Main window of the website

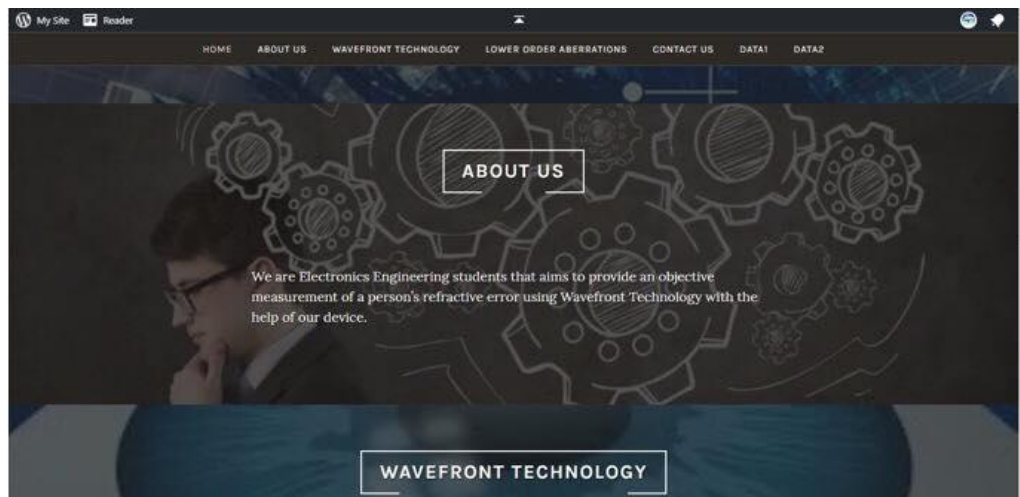


Figure 19.b Page of the website about the team



Figure 19.c Page of the website about wavefront technology

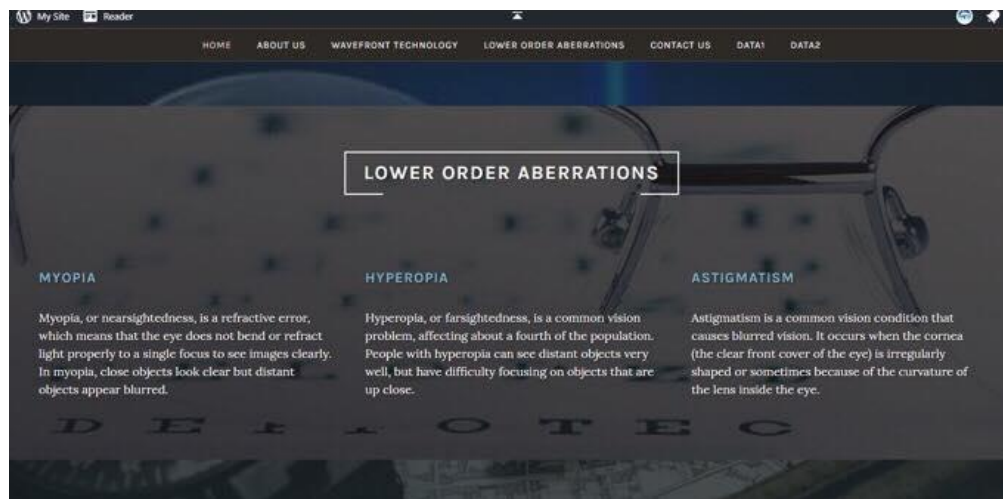


Figure 19.d Page of the website about Low Order Aberrations

File Name	SPH	CYL	AX
L201809300856	-7767.276	1462.312967	128.8719732
R201809300856	-8636.67151	1385.208298	131.371006
L201809300902	-2820.380234	776.3822794	124.8374643
R201809300902	-148.5843368	42.38174737	123.4380513
L201809300903	-163.240477	76.30664567	120.9204577
R201809300903	-225.7732967	42.08412226	127.8030577

Figure 19.e Results displayed in the website

Figures 19a-d shows the entire interface of the website. This website can be viewed online by the user. Figure 19e shows the displayed results of the lower order aberration of the user. This is updated real-time.

4.3 Project Limitation and Capabilities

This study focuses on the construction of a portable eye checkup device using wavefront aberrometry that will measure the refractive errors in the eye accurately. This study will focus on the measurement of the lower order aberrations (LOA), which include myopia, hyperopia, and astigmatism.

This study will use the principle of Shack-Hartmann for the construction of the wavefront sensor and will use Zernike polynomials and Fourier transform for the algorithm in generating the measurement of aberrations. The gathered results will be displayed on the LCD display embedded on the device itself and will also be uploaded to the website.

The device will only be limited to the identification of the lower order aberrations (LOA) that may or may not be present in the eyes and exclude the identification of the higher order aberrations (HOA) and eye diseases.

4.4 Project Evaluation

The measurements of the lower order aberrations using the device was compared to the results obtained from a clinical autorefractometer. A total of 30 samples were obtained during the eye checkup conducted. Figures 20-22 show the gathering of data through eye checkup and a sample result from the device and the clinical autorefractometer.



Figure 20. Prototype evaluation

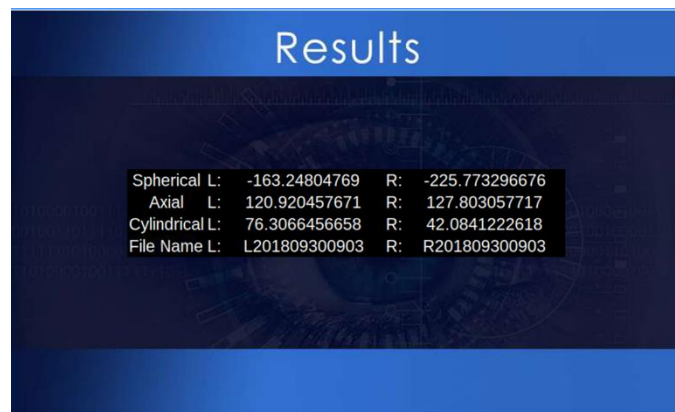


Figure 21. Result obtained from the device

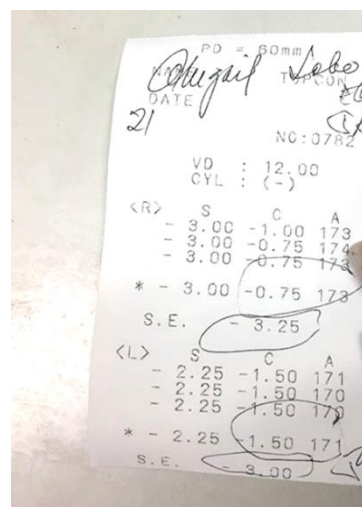


Figure 22. Result obtained from the autorefractometer

The data obtained were compared using the confusion matrix as shown in Figure 23. Since results from autorefractometers are varied up to $\pm 0.50\text{D}$ and are affected by various factors, the true positives included the yellow-shaded area of the matrix. The clinical results served as the true or actual value while the results from the algorithm for the wavefront sensor served as predicted values.

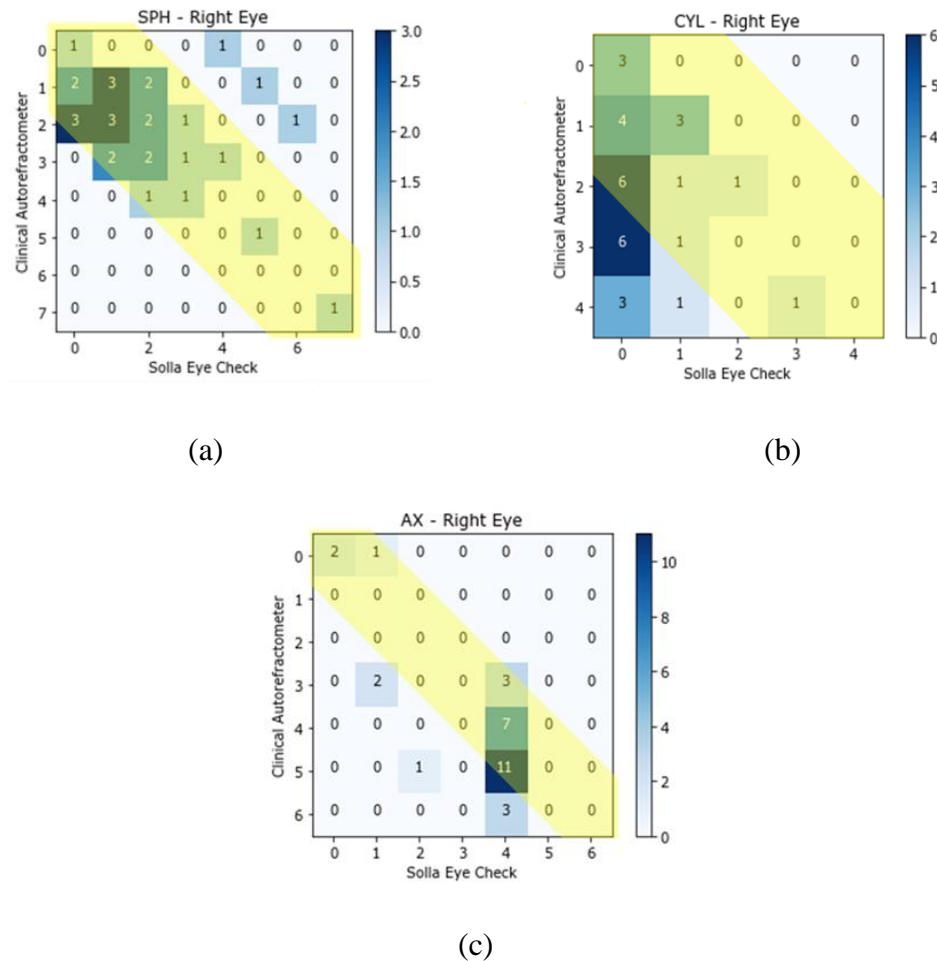


Figure 23. Confusion matrix for (a) SPH, (b) SPH, (c) AX

The accuracy, misclassification or error rate, miss rate, and fall-out rate are the measures used to analyze the confusion matrix. These measures are applicable for this

study. The accuracy rate shows what percentage of the data gathered matched the results of the clinical autorefractometer within the range of $\pm 0.50\text{D}$, while the misclassification or error rate shows the percentage that weren't in the acceptable range. The miss rate, also known as the false negative rate, shows the times that the autorefractometer has a high result but the algorithm yielded a lower result. On the other hand, the fall-out rate, also known as the false positive or false-alarm rate, shows the times that the predicted values were higher than the actual values. Tables 1-3 shows the calculated values using the different measures mentioned.

Table 2. Analysis of spherical values

Measure	Calculated Values
Accuracy	0.9
Misclassification Rate	0.1
Miss Rate	0
Fall-out	0.4286

Table 3. Analysis of cylindrical values

Measure	Calculated Values
Accuracy	0.6667
Misclassification Rate	0.3333
Miss Rate	0.3448
Fall-out	0

Table 4. Analysis of axial values

Measure	Calculated Values
Accuracy	0.8
Misclassification Rate	0.2
Miss Rate	0.6667
Fall-out	0

Based on the analysis of the confusion matrix, the accuracy of the algorithm for the wavefront sensor is about 0.7889 or 78.89% and the misclassification or error rate is about 0.2111 or 21.11%. This means that on an average, the device was able to assess the refractive errors of 24 out of 30 samples accurately. The average miss rate is 0.3371 or 33.71% and the average fall-out rate is 0.1429 or 14.29%. This means that on an average, the device predicted lower refractive errors for 10 out of 30 samples and higher refractive errors for 4 out of 30 samples.

Feedback from the users were also obtained through a survey. Figure 24 shows the results of the survey. Based on the results, the device was able to provide an easy and convenient way to conduct eye checkups. Only 4% of the users found the device difficult to use. The majority of users were also satisfied and rated the device as “above average.” Moreover, the users said they will recommend the device for conducting eye checkups.

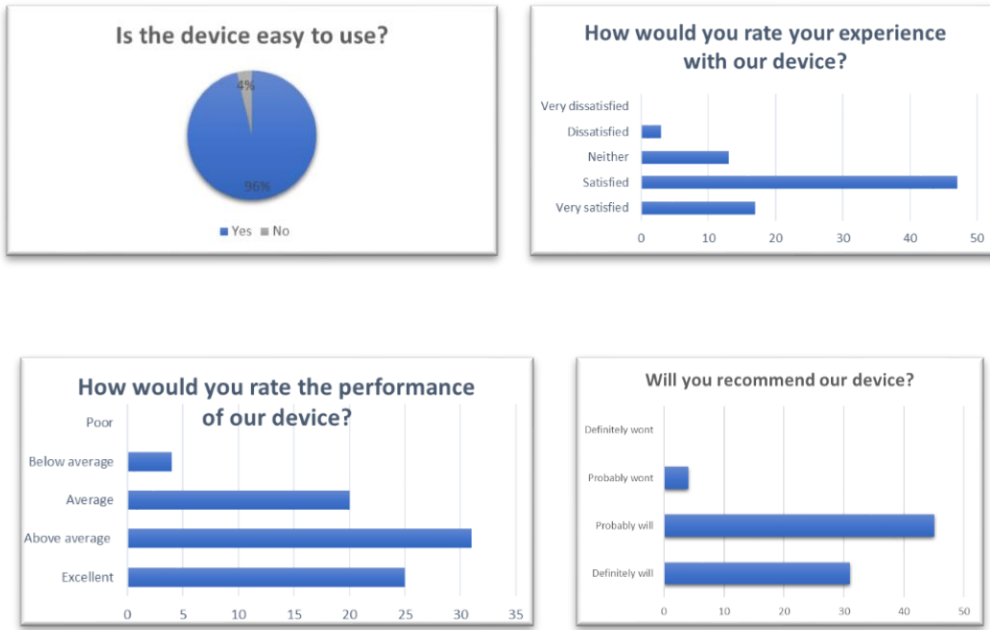


Figure 24. Survey Results

The evaluation of the accuracy and performance of the device proves that the wavefront autorefractometer developed in this study was able to deliver good results that may serve as an aid for ophthalmologists and optometrists in conducting eye checkups.

CHAPTER 5

SUMMARY OF FINDINGS, CONCLUSION, AND RECOMMENDATIONS

5.1 Summary of Findings

SOLLA Eye-Check provides accurate results in obtaining the final values of eye's aberrations. Based on the analysis of the confusion matrix, the accuracy of the algorithm for the wavefront sensor is about 0.7889 or 78.89% and the misclassification rate is about 0.2111 or 21.11%. The average miss rate is 0.3371 or 33.71% and the average fall-out rate is 0.1429 or 14.29%. Hence, the prototype may be used as the basis for eye checkups. Some factors like health conditions, time of the day and if the patient is tired may affect the results of prescriptions. Several factors, however, must be considered when conducting the eye checkup. The eyes of the user must not move during the process to provide a quality raw image. The light should also be reaching the eyes well. The user must also have enough sleep, as often recommended by ophthalmologists and optometrists since it affects the results, specifically the axial aberration.

5.2 Conclusion

1. The Shack Hartmann Wavefront sensor, that is used in this study, is composed of CCD Camera, collimating lens, visual stimulus and microlens array. The researchers acquired materials from different countries considering the cost and quality of each material and component. The case of the sensor is 3D printed and manually designed to reach the needed specifications and dimensions of the sensor to produce quality raw data

2. The devised algorithm in this study uses Zernike Polynomials and Fast Fourier Transform as core requirements that was needed to develop a program using python. With this, the program can reconstruct the captured image, generate a wavefront map and measure the refractive error.
3. The GUI displays the step by step instructions on how to properly use the device. This guides the user from the start until obtaining the result. The refractive error values can be seen through the device itself or in the website.

With the use of the device, early detection of the refractive errors in the eyes and the immediate correction using contact lenses, eyeglasses, or refractive surgeries will prevent further complications that may occur most specially to lower-aged users. Also, the device is portable and affordable compared to the commercially available aberrometers which means it can be a great help for the practitioners in the country.

5.3 Recommendations

To further improve the study, researchers recommend using a Shack-Hartmann wavefront sensor that give a high-definition image as an output. This largely affects the result of the eye checkup since the data for computations are gathered from the raw image. It is also recommended to use a better microcontroller for high-speed processing. Having a faster and easier testing by using binocular lenses where the user will have both eyes to be examined at the same time is also recommended. Furthermore, the researchers suggest that the factors affecting the eye checkups be considered. The patient should not be dizzy or tired and other light sources aside from the light reflected by the retina of the patient's eyes should be prevented from being captured by the Shack-Hartmann wavefront sensor.

REFERENCES

Jaymalin, M. (2017, August 6). *Over 2 million Pinoys blind, sight-impaired*. The Philippine Star. Retrieved March 12, 2018, from <https://www.philstar.com/headlines/2017/08/06/1726085/over-2-million-pinoys-blindsight-impaired>

Mirko Resan, Miroslav Vukosavljević and Milorad Milivojević (2012). *Wavefront Aberrations*, Advances in Ophthalmology, Dr Shimon Rumelt (Ed.), InTech, DOI: 10.5772/24441

Uncorrected Refractive Error. (n.d.). Retrieved March 12, 2018, from <http://www.lcif.org/EN/our-work/sight/uncorrected-refractive-error.php>

Eye exam. (2017, December 29). Retrieved March 12, 2018, from <https://www.mayoclinic.org/tests-procedures/eye-exam/about/pac-20384655>

De Leon, A. S. (March 2004). *The Blind Filipino: What have we done? What needs to be done?* Philippine Journal of Ophthalmology, 29(1), 42-52.

Vessel, M., & Heiting, OD., G. (2016, January). *Wavefront Technology in Eye Exams*. Retrieved March 12, 2018, from <http://www.allaboutvision.com/eyeeexam/wavefront.htm>

Resnikoff, S., Felch, W., Gauthier, T., & Spivey, B. (2012). *The number of ophthalmologists in practice and training worldwide: a growing gap despite more than 200 000 practitioners*. British Journal of Ophthalmology, 96:783-787.

- Manneberg, Otto. (2018). *Design and Simulation of a High Spatial Resolution Hartmann-Shack Wavefront Sensor*. Stockholm, Sweden: Royal Institute of Technology.
- Heiting, G. (n.d.). *How to Read Your Eyeglass Prescription*. Retrieved March 17, 2018, from <http://www.allaboutvision.com/eyeglasses/eyeglass-prescription.htm>
- Platt, B. C., & Shack, R. (2001). *History and Principles of Shack-Hartmann Wavefront Sensing*. Journal of Refractive Surgery, 17, S573-S577.
- Juergens, R. (n.d.). *OPTI 517 Image Quality*. Lecture. Retrieved March 12, 2018, from <https://wp.optics.arizona.edu/jsasian/wp-content/uploads/sites/33/2016/02/Opti517-Optical-Quality-2017.pdf>
- Guirao, A., & Williams, A. D. (2003). *A Method to Predict Refractive Errors from Wave Aberration Data*. Optometry and Vision Science, 80(1), 36-42.
doi:10.1097/00006324-200301000-00006
- Thibos, L. N., (2003, February). *Representation of Wavefront Aberrations*. Retrieved from
<http://voi.opt.uh.edu/VOI/WavefrontCongress/2003/presentations/Thibos/Shortcourse.pdf>
- What is Visual Design?* (n.d.). Retrieved from
<https://www.interactiondesign.org/literature/topics/visual-design>
- What is mobile app security?* - Definition from WhatIs.com. (n.d.). Retrieved from <http://whatis.techtarget.com/definition/mobile-app-security>

Core app quality. (2018, March 07). Retrieved from
<https://developer.android.com/develop/quality-guidelines/core-app-quality.html#ps>

Refractive errors in Filipino eyes in a single-center study population. (n.d.).
Retrieved March 24, 2018, from <http://www.paojournal.com/vol35no2/refractive.php>

Paojournal.com. (n.d.). Retrieved March 23, 2018, from
<http://paojournal.com/archives/vol36no1/vol36no1/article2.php&p=DevEx,5061.1>

Comparison in the quality of vision and spherical ... (n.d.). Retrieved March 23, 2018, from

http://www.paojournal.com/xml/pjo2012_vol33no1/pdfs/5.pdf&p=DevEx,5066.1

Refractive errors in Filipino eyes in a single-center study population. (n.d.).
Retrieved March 24, 2018, from <http://www.paojournal.com/vol35no2/refractive.php>

A simple and effective algorithm for detection of arbitrary Hartmann–Shack patterns. (2003, December 03). Retrieved March 24, 2018, from
<https://www.sciencedirect.com/science/article/pii/S1532046403001138>

The 2012 Charles Prentice Medal Lecture: Wavefront ... (n.d.). Retrieved March 23, 2018, from

http://journals.lww.com/optvissci/fulltext/2013/09000/the_2012_charles_prentice_medal_lecture__.4.aspx&p=DevEx,5070.1

A Comparison of a Traditional and Wavefront Autorefraction ... (n.d.). Retrieved March 23, 2018, from

https://www.researchgate.net/publication/265419448_A_Comparison_of_a_Traditional_and_Wavefront_Autorefraction&p=DevEx,5068.1

Cade, F., Cruzat, A., Paschalis, E., Espírito Santo, L., & Pineda, R. (2013). *Analysis of Four Aberrometers for Evaluating Lower and Higher Order Aberrations*. Plos ONE, 8(1), e54990. doi: 10.1371/journal.pone.0054990

Carvalho, L. (2005). *Accuracy of Zernike Polynomials in Characterizing Optical Aberrations and the Corneal Surface of the Eye*. Investigative Ophthalmology & Visual Science, 46(6), 1915. doi: 10.1167/iovs.04-1222

Eye exam - Mayo Clinic. (2018). Retrieved from
<https://www.mayoclinic.org/tests-procedures/eye-exam/about/pac-20384655>

Facts About Refractive Errors / National Eye Institute. (2010). Retrieved from
<https://nei.nih.gov/health/errors/errors>

Lombardo, M., & Lombardo, G. (2009). *New methods and techniques for sensing the wave aberrations of human eyes*. Clinical And Experimental Optometry, 92(3), 176-186. doi: 10.1111/j.1444-0938.2009.00356.x

Parthasarathy, M., & Lakshminarayanan, V. (2017). *A Brief History of Aberrometry Applications in Ophthalmology and Vision Science*. Springer Proceedings In Physics, 31-39. doi: 10.1007/978-981-10-3908-9_4

Resan, M., Vukosavljevi, M., & Milivojevi, M. (2012). *Wavefront Aberrations*. Advances In Ophthalmology. doi: 10.5772/24441

Schwiegerling, J. (2014). *History of the Shack Hartmann wavefront sensor and its impact in ophthalmic optics*. Fifty Years Of Optical Sciences At The University Of Arizona. doi: 10.11117/12.2064536

Schwiegerling, J., & Neal, D. (2005). *Historical Development of the Shack-Hartmann Wavefront Sensor* [Ebook]. Retrieved from
https://www.researchgate.net/publication/241520304_Historical_Development_of_the_Shack-Hartmann_Wavefront_Sensor

Uncorrected Refractive Error / Lions Clubs International. (2019). Retrieved from
<https://lionsclubs.org/en/resources-for-members/resource-center/uncorrected-refractive-error>

Vision impairment and blindness. (2018). Retrieved from
<https://www.who.int/news-room/fact-sheets/detail/blindness-and-visual-impairment>

Wallerstein, A. (2016). *Aberrometry and Wavefront Imaging: Historical Perspective, Wavefront Error, Optical Aberrations of the Eye*. Retrieved from
<https://emedicine.medscape.com/article/1228601-overview>

Wavefront Technology is the Wave of the Future. (2016). [Blog]. Retrieved from
<https://www.smartvisionlabs.com/blog/wavefront-technology-is-the-wave-of-the-future/>

World Health Organization. (2013). *Universal eye health*. Geneva.

Yoon, G., Pantanelli, S., & Macrae, S. (2007). *Comparison of Zernike and Fourier wavefront reconstruction algorithms in representing the corneal aberration of normal and abnormal eyes*. Journal Of Refractive Surgery, (24), 582-90.

Basic evaluation measures from the confusion matrix. (2015). Retrieved from
<https://classeval.wordpress.com/introduction/basic-evaluation-measures/>

Beverage, J. (2003). *Measuring refractive error in the human eye using a Shack-Hartmann-based autorefractor* (Ph.D., Doctoral). University of Arizona.

Jesson, M., Pachiyappan, A., & Ganesan, A. (2019). *Analysis of Refractive errors in the human eye using Shack Hartmann Aberrometry* [Ebook]. Retrieved from
https://www.researchgate.net/publication/266471430_Analysis_of_Refraetive_errors_in_the_human_eye_using_Shack_Hartmann_Aberrometry

Maeda, N. (2009). *Clinical applications of wavefront aberrometry - a review*. Clinical & Experimental Ophthalmology, 37(1), 118-129. doi: 10.1111/j.1442-9071.2009.02005.x

Maeda, P. (2003). *"Zernike polynomials and their use in describing the wavefront aberrations of the human eye*. Stanford University.

Mishra, M. (2018). *Simplifying The Confusion Matrix – Data Driven Investor – Medium*. Retrieved from <https://medium.com/datadriveninvestor/simplifying-the-confusion-matrix-aa1fa0b0fc35>

Smoothing Images — OpenCV 2.4.13.7 documentation. (2019). Retrieved from
https://docs.opencv.org/2.4/doc/tutorials/imgproc/gaussian_median.blur_bilateral.filter/gaussian_median.blur_bilateral.filter.html

Strang, N., Gray, L., Winn, B., & Pugh, J. (1998). *Clinical evaluation of patient tolerance to autorefractor prescriptions*. Clinical And Experimental Optometry, 81(3), 112-118. doi: 10.1111/j.1444-0938.1998.tb06729.x

You Can Visit Two Eye Doctors and Get TWO Different Prescriptions, Here's Why. (2018). [Blog]. Retrieved from <https://www.eyeque.com/knowledge-center/you-can-visit-two-eye-doctors-and-get-two-different-prescriptions-heres-why/>

Optica Tehnica. (2004) *University of Oradea Editor*. ISBN 973-673-590-X, Oradea.

ZECCHINO, M (2003). *Measuring Micro-Lens Radius of Curvature with a White Light Optical Profiler*. Veeco Instruments Inc.-Catalog, pp.1-2, USA, AN509-Measuring-05213lr.pdf

A. Pop (2007). *Applications of Microlenses Array*. Retrieved from https://www.researchgate.net/profile/Petru_Pop/publication/267382565_Applications_of_Microlens_Arrays/links/545a4ef50cf2c46f66426dff/Applications-of-Microlens-Arrays.pdf

B. S. Valentina, B. Ramona, S. Speranta & T. Calin. *The influence of optical aberrations in refractive surgery*. Retrieved from <https://www.ncbi.nlm.nih.gov/pmc/articles/PMC5712942/>

(03-Dec-2003) *A simple and effective algorithm for detection of arbitrary Hartmann-Shack patterns*. NeuroImage, Retrieved from <https://www.sciencedirect.com/science/article/pii/S1532046403001138>.

J. Porter. (2006). *Adaptive Optics for Vision Science Principles, Practices, Design and Applications*. Canada: JOHN WILEY & SONS, INC.

U. Levi (2017). *Limitation in Peripheral Optics Measurement of the Eye*. Master's thesis, Queensland University of Technology, Retrieved from
doi:10.5204/thesis.eprints.109469

G. Bailey. *Myopia(Nearsightedness): Causes and Treatment*, [Blog] Retrieved from <https://www.allaboutvision.com/conditions/myopia.htm>

G. Bailey. *Hyperopia(Farsightedness)*. [Blog] Retrieved from
<https://www.allaboutvision.com/conditions/hyperopia.htm>

M. Resan, M. Vukosavljević, and M. Milivojević. “*Wavefront Aberrations, Advances in Ophthalmology, Dr Shimon Rumelt (Ed)*”. Retrieved from
<http://www.intechopen.com/books/advances-in-ophthalmology/wavefront-aberrations>

M. Vessel. "Higher-Order Aberrations" [Blog] Retrieved from
<https://www.allaboutvision.com/conditions/aberrations.htm>

B. S. Valentina, B. Ramona, S. Speranta & T. Calin. “*The influence of optical aberrations in refractive surgery*” Retrieved from
<https://www.ncbi.nlm.nih.gov/pmc/articles/PMC5712942/>

A. Wallerstein. "Wavefront-Guided Refractive Surgery" Retrieved from
https://www.lasikmd.com/documents/wavefront_guided_refractive_surgery.pdf

APPENDIX A

Needs Assessment

The proponents prepared a survey that is composed of eight questions mainly about the importance of autorefractor in performing eye checkups. The respondents of this survey were ophthalmologist from different hospitals in Metro Manila, Philippines. A total of 16 surveys were collected and the results of which are analyzed in this Appendix. The purpose of the survey is to attest the importance of autorefractor and to see if it will be helpful for the field of optometry and ophthalmology to have a portable autorefractor. Survey results are depicted on the following pages.

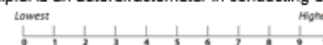
	Technological University of the Philippines Ayala Blvd., Ermita, Manila College of Engineering Electronics Engineering Department	
---	---	---

Name: _____ Contact No.: _____

Subject: "Measurement of Lower-Order Aberrations in the Eyes Using Wavefront Aberrometry Based on a CCD Camera Accompanied by an Android App"

Questions:

- How helpful is an autorefractometer in conducting eye checkups?


- Should all eye clinics have at least one autorefractometer?
 Yes No
- How much does a typical autorefractometer cost?

- Do you conduct community service/free eye checkups in different areas aside from an eye clinic?
 Yes No
- If yes, do you bring an autorefractometer with you?
 Yes No
- How hassle is it to bring an autorefractometer?


- What are the limitations of an autorefractometer?

- Will a portable & low-cost aberrometer, which may be used by all ages, be helpful in the field of optometry and ophthalmology?
 Yes No

Thank you for being a part of our survey. Have a nice day! :)

Figure 1. Survey Form

SURVEY RESULTS

1. How helpful is an autorefractometer in conducting eye checkup?

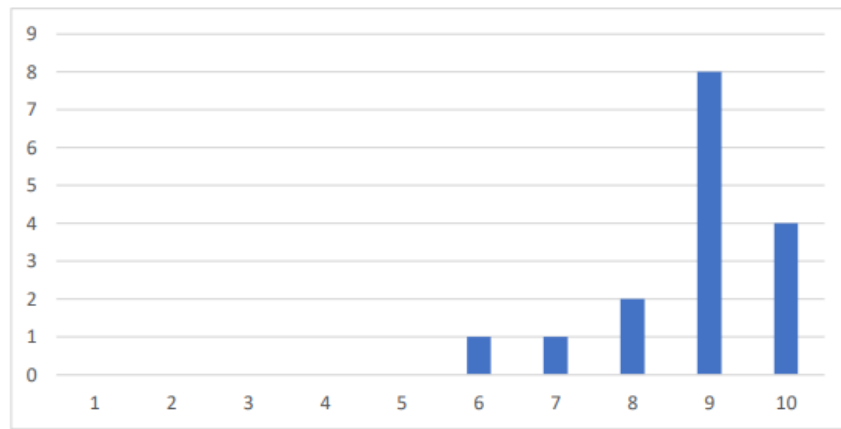


Figure 2

2. Should all eye clinics have at least one autorefractometer?



Figure 3

3. How much does a typical autorefractometer cost?

Range Based on their answers: Php 100 000 – Php 500 000

4. Do you conduct community service/free eye checkups in different areas aside from an eye clinic?



Figure 4

5. If yes, do you bring an autorefractometer with you?



Figure 5

6. How hassle is it to bring an autorefractometer?

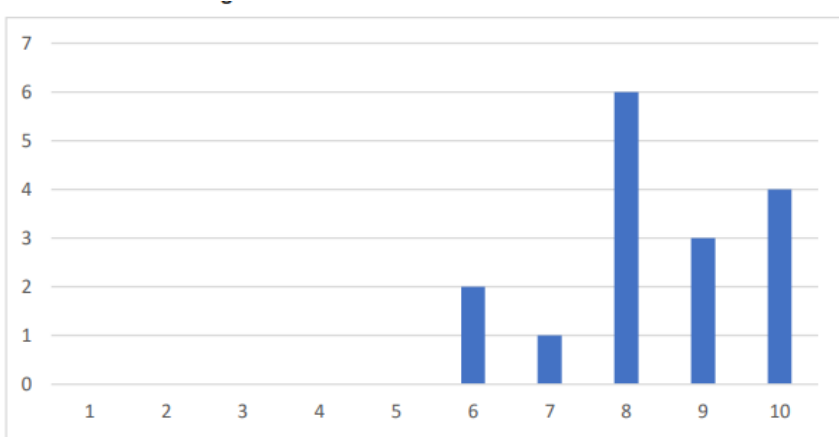


Figure 6

7. What are the limitations of an autorefractometer?

The autorefractometer is large and heavy, making it difficult and hassle to bring. It is also expensive. It may not be used by pediatric patients. The result's consistency also varies.

8. Will a portable & low cost aberrometer, which may be used by all ages, be helpful in the field of optometry and ophthalmology?



Figure 7

The results showed the importance of autorefractometer in performing eye checkups. Having a portable autorefractometer will be a great help in the field of optometry and ophthalmology most especially during eye checkups outside clinics or hospitals where they must carry bulky and heavyweight autorefractors.

APPENDIX B

Program Codes

```
from guizero import App, Combo, Text, CheckBox, ButtonGroup, Box, Picture, yesno,  
Window, PushButton, info, TextBox, ListBox  
  
  
import datetime  
import picamera  
import time  
import cv2  
import numpy as np  
  
  
def open_instructions():  
    instructions.show(wait=True)  
    app.hide()  
  
  
def open_window():  
    left.show(wait=True)  
    instructions.hide()  
  
  
def close_window():  
    left.hide()  
    right.hide()  
  
  
'App'  
app= App(title="SOLLA", width=800, height=480,bg="white")
```

```

open_button = Picture(app, image="first.png")
open_button.when_clicked = open_instructions

'Instructions'
instructions= Window(app, title="SOLLA", width=800, height=480, layout="grid",
bg="white")
instructions.hide()
instructionbg=Picture(instructions, grid=[0,0],image="instructionss.png")
instructionbg.when_clicked= open_window

def open_right():
    right.show()
    left.hide()
    d = datetime.datetime.now()
    imgYear = "%04d" % (d.year)
    imgMonth = "%02d" % (d.month)
    imgDate = "%02d" % (d.day)
    imgHour = "%02d" % (d.hour)
    imgMins = "%02d" % (d.minute)
    fileNameL = 'L'+ str(imgYear) + str(imgMonth) + str(imgDate) + str(imgHour) +
    str(imgMins)
    fileName = '/home/pi/Desktop/SOLLABO/images/L' + str(imgYear) + str(imgMonth)
    + str(imgDate) + str(imgHour) + str(imgMins) + '.jpg'

```

```
cameraleft = picamera.PiCamera()  
  
cameraleft.start_preview()  
  
time.sleep(10)  
  
cameraleft.capture(fileName)  
  
cameraleft.stop_preview()  
  
cameraleft.close()
```

```
# Import necessary packages  
  
import cv2  
  
import numpy as np  
  
  
# Load image and crop  
  
imageL = cv2.imread(fileName)  
  
y = 270  
  
h = 150  
  
x = 350  
  
w = 150  
  
cimage1 = imageL[y:y+h, x:x+w]
```

```
# Save as PNG  
  
from PIL import Image  
  
im.value = Image.fromarray(cimage1)
```

```

# Convert to greyscale and enhance edges

gray1 = cv2.cvtColor(cimage1, cv2.COLOR_BGR2GRAY)

gray1 = cv2.GaussianBlur(gray1,(5,5),0);

gray1 = cv2.medianBlur(gray1,5)

# Fourier transform

f1 = np.fft.fft2(gray1)

# Apply shift to place DC component in the center

fshift1 = np.fft.fftshift(f1)

# Power magnitude spectrum of the fft

magspec1 = 20*np.log(np.abs(fshift1))

# Phase Spectrum of the fft

phase1 = np.angle(fshift1)

# Constants

pupilsize = 6

# Magnitude and Phase

rhoL = np.abs(pkL1-pkL2)

thetaL = np.abs(pkL3-pkL4)

```

```

# Zernike Coefficients

z1 = 2*np.square(rhoL)-1

z2 = np.square(rhoL)*np.cos(2*thetaL);

z3 = np.square(rhoL)*np.sin(2*thetaL);

# Convert to meters

z1 = z1/10**6;

z2 = z2/10**6;

z3 = z3/10**6;

# Computation : Left Eye

if (z3==0):

    alphaL = (-1)*np.sign(z1)*np.pi/4; #special case when z3 is equal to zero

else:

    alphaL = (-1)*0.5*np.arctan(z1/z3);

if (abs(z3)<abs(z1)):

    AL = z1*2*np.sqrt(6)/np.sin(2*alphaL);

else:

    AL = -z3*2*np.sqrt(6)/np.cos(2*alphaL);

```

```

axL = (-1)*180*alphaL/np.pi; # AXIAL

if (AL<=0):
    AL = (-1)*AL;
    axL = axL-90;
    if (axL<=0):
        axL = axL+180;

DL = z2*2*np.sqrt(3)-AL/2;
cylL= -20*DL/((pupilsize/2000)**2); # CYLINDRICAL
sphL = -20*AL/((pupilsize/2000)**2); # SPHERICAL

cylLeft.value=str(cylL)
sphLeft.value=str(sphL)
axLeft.value=str(axL)
raw_fileNameL.value=str(fileNameL)

import gspread
from oauth2client.service_account import ServiceAccountCredentials
scope = ['https://spreadsheets.google.com/feeds' ,
'https://www.googleapis.com/auth/drive']
credentials = ServiceAccountCredentials.from_json_keyfile_name('SOLLABO-
EyecheckUp-5d59553c9325.json', scope)

```

```

gc = gspread.authorize(credentials)

wks = gc.open('SOLLABO_Results').sheet1

wks.append_row([fileNameL, sphL, cylL, axL])

'LEFT'

left=Window(instructions, title="SOLLA", width=800, height=480, layout="grid",
bg="snow")

left.hide()

box = Box(left,layout="grid", grid=[0,0])

hehestry=Box(box, grid=[0,0])

push=PushButton(box,image="left.png", command=open_right, grid=[0,0])

Pictureha=Picture(hehestry, image="Latestbg.png" ,grid=[0,1])



def open_showresults():

    showresults.show()

    right.hide()

d1 = datetime.datetime.now()

imgYear1 = "%04d" % (d1.year)

imgMonth1 = "%02d" % (d1.month)

imgDate1 = "%02d" % (d1.day)

```

```

imgHour1 = "%02d" % (d1.hour)

imgMins1 = "%02d" % (d1.minute)

fileNameR = 'R'+ str(imgYear1) + str(imgMonth1) + str(imgDate1) + str(imgHour1) +
str(imgMins1)

fileName1 = '/home/pi/Desktop/SOLLABO/images/R' + str(imgYear1) +
str(imgMonth1) + str(imgDate1) + str(imgHour1) + str(imgMins1) + '.jpg'

cameraright = picamera.PiCamera()

cameraright.start_preview()

time.sleep(10)

cameraright.capture(fileName1)

cameraright.stop_preview()

cameraright.close()

# Import necessary packages

import cv2

import numpy as np

# Load image and crop

imageR = cv2.imread(fileName1)

y = 270

h = 150

x = 350

w = 150

```

```

cimage2 = imageR[y:y+h, x:x+w]

# Save as PNG

from PIL import Image

im1.value = Image.fromarray(cimage2)

# Convert to greyscale and enhance edges

gray2 = cv2.cvtColor(cimage2, cv2.COLOR_BGR2GRAY)

gray2 = cv2.GaussianBlur(gray2,(5,5),0);

gray2 = cv2.medianBlur(gray2,5)

# Fourier transform

f2 = np.fft.fft2(gray2)

# Apply shift to place DC component in the center

fshift2 = np.fft.fftshift(f2)

# Power magnitude spectrum of the fft

magspec2 = 20*np.log(np.abs(fshift2))

# Phase Spectrum of the fft

phase2 = np.angle(fshift2)

```

```

# Constants

pupilsize = 6


# Magnitude and Phase

rhoR = np.abs(pkR1-pkR2)

thetaR = np.abs(pkR3-pkR4)


# Zernike Coefficients

zR1 = 2*np.square(rhoR)-1

zR2 = np.square(rhoR)*np.cos(2*thetaR);

zR3 = np.square(rhoR)*np.sin(2*thetaR);


# Convert to meters

zR1 = zR1/10**6;

zR2 = zR2/10**6;

zR3 = zR3/10**6;


# Computation : Right Eye

if (zR3==0):

    alphaR = (-1)*np.sign(zR1)*np.pi/4; #special case when z3 is equal to zero

else:

    alphaR = (-1)*0.5*np.arctan(zR1/zR3);

```

```

if (abs(zR3)<abs(zR1)):

    AR = zR1*2*np.sqrt(6)/np.sin(2*alphaR);

else:

    AR = -zR3*2*np.sqrt(6)/np.cos(2*alphaR);

axR = (-1)*180*alphaR/np.pi; #AXIAL

if (AR<=0):

    AR = (-1)*AR;

    axR = axR-90;

if (axR<=0):

    axR = axR+180;

DR = zR2*2*np.sqrt(3)-AR/2;

cylR = -20*DR/((pupilsiz/2000)**2); # CYLINDRICAL

sphR = -20*AR/((pupilsiz/2000)**2); # SPHERICAL

raw_fileNameR.value=str(fileNameR)

cylRight.value=str(cylR)

sphRight.value=str(sphR)

axRight.value=str(axR)

import gspread

```

```

from oauth2client.service_account import ServiceAccountCredentials
scope = ['https://spreadsheets.google.com/feeds' ,
'https://www.googleapis.com/auth/drive']
credentials = ServiceAccountCredentials.from_json_keyfile_name('SOLLABO-
EyecheckUp-5d59553c9325.json', scope)
gc = gspread.authorize(credentials)
wks = gc.open('SOLLABO_Results').sheet1
wks.append_row([fileNameR, sphR, cylR, axR])

```

'RIGHT'

```

right=Window(left, title="SOLLA", width=800, height=480, layout="auto", bg="white")
right.hide()
boxr = Box(right,layout="grid", grid=[0,0])
hehestryr=Box(boxr, grid=[0,0])
pushr=PushButton(boxr,image="right.png", command=open_showresults, grid=[0,0])
Picturehar=Picture(hehestryr, image="Latestbg.png" ,grid=[0,1])

```

```

def open_results():
    showresults.hide()
    results.show()

```

```

'Show Results'

showresults=Window(right, title="Show Results", width=800, height=480,
layout="grid", bg="black")

showresults.hide()

firstboxpic=Box(showresults, layout="grid", grid=[0,0])

show=Picture(firstboxpic,image="pictureresults.png", grid=[0,0])

show.when_clicked= open_results

secondboxpic=Box(firstboxpic, layout="grid", grid=[0,0])

im=Picture(secondboxpic, grid=[0,0])

im1=Picture(secondboxpic, grid=[1,0])



def new():

    results.hide()

    app.show()

#cv2.imshow("output,np.hstack([image, output])"

'Results'

results=Window(showresults, title="SOLLA", width=800, height=480, layout="grid",
bg="white")

```

```

results.hide()

firstbox=Box(results, layout="grid", grid=[0,0])

background=Picture(firstbox, image="results.png", grid=[0,0])

secondbox=Box(firstbox, layout="grid", grid=[0,0])

secondbox.bg="black"

spherical=Text(secondbox, text="Spherical", size="15", grid=[0,0], color="white")

sphl=Text(secondbox, text="L:", size="15", grid=[1,0], color="white")

sphr=Text(secondbox, text="R:", size="15", grid=[3,0], color="white")

sphLeft=Text(secondbox, text="-", size="15", grid=[2,0], color="white")

sphRight=Text(secondbox, text="-", size="15", grid=[4,0], color="white")

sphLeft.width="17"

sphLeft.text_color="white"

sphLeft.text_size=15

sphRight.width="17"

sphRight.text_color="white"

sphRight.text_size=15

axial=Text(secondbox, text="Axial", size="15", grid=[0,1], color="white")

axl=Text(secondbox, text="L:", size="15", grid=[1,1], color="white")

axr=Text(secondbox, text="R:", size="15", grid=[3,1], color="white")

axLeft=Text(secondbox, text="-", size="15", grid=[2,1], color="white")

```

```
axRight=Text(secondbox, text="-", size="15", grid=[4,1], color="white")
axLeft.width="17"
axLeft.text_color="white"
axLeft.text_size=15
axRight.width="17"
axRight.text_color="white"
axRight.text_size=15

cylindrical=Text(secondbox, text="Cylindrical",size="15", grid=[0,2],color="white")
cylL=Text(secondbox, text="L:", size="15", grid=[1,2], color="white")
cylR=Text(secondbox, text="R:", size="15", grid=[3,2], color="white")
cylLeft=Text(secondbox, text="-", size="15", grid=[2,2], color="white")
cylRight=Text(secondbox, text="-", size="15", grid=[4,2], color="white")
cylLeft.text_color="white"
cylLeft.width="17"
cylLeft.text_size=15
cylRight.text_color="white"
cylRight.width="17"
cylRight.text_size=15

filename=Text(secondbox, text="File Name", size="15", grid=[0,3], color="white")
fileNamel=Text(secondbox, text="L:", size="15", grid=[1,3], color="white")
```

```
fileNamer=Text(secondbox, text="R:", size="15", grid=[3,3], color="white")
raw_fileNameL=Text(secondbox, text="-", size="15", grid=[2,3],color="white")
raw_fileNameR=Text(secondbox, text="-", size="15", grid=[4,3],color="white")
#fileNameL=TextBox(secondbox, text="-", grid=[2,3])
#fileNameR=TextBox(secondbox, text="-", grid=[4,3])

#fileNameL.text_color="white"
#fileNameL.width="17"
#fileNameL.text_size=20
#fileNameR.text_color="white"
#fileNameR.width="17"
#fileNameR.text_size=20
background.when_clicked= new
app.display()
```

APPENDIX C

Bill of Materials

Bill of Materials

MATERIALS	COST
Collimating Lens	₱338.60
Microlens Array	₱24,800.00
Raspberry Pi 3	₱2,400.00
SD Card	₱1,000.00
Camera Module	₱1,650.00
Raspberry Pi 3 - Screen	₱2,500.00
USB Cord - CDR KING	₱30.00
Switch	₱25.00
Eye cup	₱350.00
3D PRINT - Base	₱5,000.00
3D Print - Top	₱3,100.00
USB Cord	₱149.00
Jaguar Power bank	₱550.00
Resistor, Screw, LED	₱50.00
TOTAL	₱41,942.60

APPENDIX D

Specifications and Datasheets

SOLLA EYECHECK SPECIFICATIONS

Length	130mm
Width	280mm
Height	125mm
Sensor weight	10lbs
Array size and type	10x10mm, square grid
Lens pitch	150 µm
Lens diameter	146 µm
Focal length	5.2mm
Camera resolution	8megapixel, 3280x2464pixel
Led wavelength	700nm
Operating hours	24-30 hours
Operating system	Raspberry pi

RASBERRY PI 3B



Farnell

element14

<http://uk.farnell.com/buy-raspberry-pi>



Newark

element14

<http://www.newark.com/buy-raspberry-pi>

Technical Specification:

Processor

- Broadcom BCM2387 chipset.
- 1.2GHz Quad-Core ARM Cortex-A53 (64Bit)

802.11 b/g/n Wireless LAN and Bluetooth 4.1 (Bluetooth Classic and LE)

- IEEE 802.11 b / g / n Wi-Fi. Protocol: WEP, WPA WPA2, algorithms AES-CCMP (maximum key length of 256 bits), the maximum range of 100 meters.
- IEEE 802.15 Bluetooth, symmetric encryption algorithm Advanced Encryption Standard (AES) with 128-bit key, the maximum range of 50 meters.

GPU

- Dual Core Video Core IV® Multimedia Co-Processor. Provides Open GL ES 2.0, hardware-accelerated Open VG, and 1080p30 H.264 high-profile decode.
- Capable of 1Gpixel/s, 1.5Gtexel/s or 24GFLOPs with texture filtering and DMA infrastructure

Memory

- 1GB LPDDR2

Operating System

- Boots from Micro SD card, running a version of the Linux operating system or Windows 10 IoT

Dimensions

- 85 x 56 x 17mm

Power

- Micro USB socket 5V1, 2.5A

Connectors:

Ethernet

- 10/100 BaseT Ethernet socket

Video Output

- HDMI (rev 1.3 & 1.4)
- Composite RCA (PAL and NTSC)

Audio Output

- Audio Output 3.5mm jack
- HDMI
- USB 4 x USB 2.0 Connector

GPIO Connector

- 40-pin 2.54 mm (100 mil) expansion header: 2x20 strip
- Providing 27 GPIO pins as well as +3.3 V, +5 V and GND supply lines

Camera Connector

- 15-pin MIPI Camera Serial Interface (CSI-2)

Display Connector

- Display Serial Interface (DSI) 15 way flat flex cable connector with two data lanes and a clock lane

Memory Card Slot

- Push/pull Micro SDIO



<http://uk.farnell.com/buy-raspberry-pi>



<http://www.newark.com/buy-raspberry-pi>

The GPU provides Open GL ES 2.0, hardware-accelerated Open VG, and 1080p30 H.264 high-profile decode and is capable of 1Gpixel/s, 1.5Gtexel/s or 24 GFLOPs of general purpose compute. What's that all mean? It means that if you plug the Raspberry Pi 3 into your HDTV, you could watch BluRay quality video, using H.264 at 40MBits/s



The biggest change that has been enacted with the Raspberry Pi 3 is an upgrade to a next generation main processor and improved connectivity with Bluetooth Low Energy (BLE) and BCM43143 Wi-Fi on board. Additionally, the Raspberry Pi 3 has improved power management, with an upgraded switched power source up to 2.5 Amps, to support more powerful external USB devices.





<http://uk.farnell.com/buy-raspberry-pi>



<http://www.newark.com/buy-raspberry-pi>

The Raspberry Pi 3's four built-in USB ports provide enough connectivity for a mouse, keyboard, or anything else that you feel the RPi needs, but if you want to add even more you can still use a USB hub. Keep in mind, it is recommended that you use a powered hub so as not to overtax the on-board voltage regulator. Powering the Raspberry Pi 3 is easy, just plug any USB power supply into the micro-USB port. There's no power button so the Pi will begin to boot as soon as power is applied, to turn it off simply remove power. The four built-in USB ports can even output up to 1.2A enabling you to connect more power hungry USB devices (This does require a 2Amp micro USB Power Supply)



On top of all that, the low-level peripherals on the Pi make it great for hardware hacking. The 0.1" spaced 40-pin GPIO header on the Pi gives you access to 27 GPIO, UART, I²C, SPI as well as 3.3 and 5V sources. Each pin on the GPIO header is identical to its predecessor the Model B+.

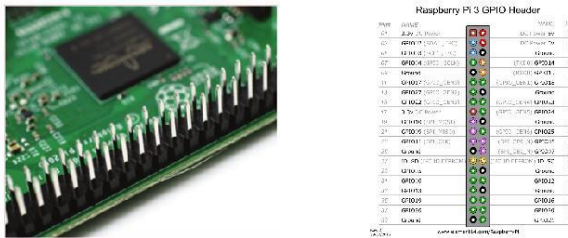
SoC

Built specifically for the new Pi 3, the Broadcom BCM2837 system-on-chip (SoC) includes four high-performance ARM Cortex-A53 processing cores running at 1.2GHz with 32kB Level 1 and 512kB Level 2 cache memory, a VideoCore IV graphics processor, and is linked to a 1GB LPDDR2 memory module on the rear of the board.



GPIO

The Raspberry Pi 3 features the same 40-pin general-purpose input-output (GPIO) header as all the Pis going back to the Model B+ and Model A+. Any existing GPIO hardware will work without modification; the only change is a switch to which UART is exposed on the GPIO's pins, but that's handled internally by the operating system.



USB chip

The Raspberry Pi 3 shares the same SMSC LAN9514 chip as its predecessor, the Raspberry Pi 2, adding 10/100 Ethernet connectivity and four USB channels to the board. As before, the SMSC chip connects to the SoC via a single USB channel, acting as a USB-to-Ethernet adaptor and USB hub.



Antenna

There's no need to connect an external antenna to the Raspberry Pi 3. Its radios are connected to this chip antenna soldered directly to the board, in order to keep the size of the device to a minimum. Despite its diminutive stature, this antenna should be more than capable of picking up wireless LAN and Bluetooth signals – even through walls.



Key Improvements from Pi 2 Model B to Pi 3 Model B:

- Next Generation QUAD Core Broadcom BCM2837 64bit ARMv7 processor
- Processor speed has increased from 900MHz on Pi 2 to 1.25Ghz on the RPi 3 Model B
- BCM43143 Wi-Fi on board
- Bluetooth Low Energy (BLE) on board
- Upgraded switched power source up to 2.5 Amps (can now power even more powerful devices over USB ports)

The main differences are the quad core 64-bit CPU and on-board Wi-Fi and Bluetooth. The RAM remains 1GB and there is no change to the USB or Ethernet ports. However, the upgraded power management should mean the Pi 3 can make use of more power hungry USB devices

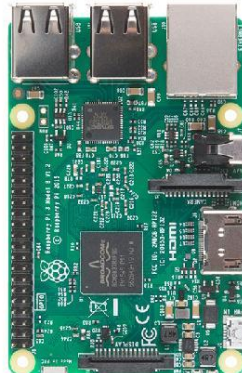
For Raspberry Pi 3, Broadcom have supported us with a new SoC, BCM2837. This retains the same basic architecture as its predecessors BCM2835 and BCM2836, so all those projects and tutorials which rely on the precise details of the Raspberry Pi hardware will continue to work. The 900MHz 32-bit quad-core ARM Cortex-A7 CPU complex has been replaced by a custom-hardened 1.2GHz 64-bit quad-core ARM Cortex-A53

In terms of size it is identical to the B+ and Pi 2. All the connectors and mounting holes are in the same place so all existing add-ons, HATs and cases should fit just fine although the power and activity LEDs have moved to make room for the WiFi antenna.

The performance of the Pi 3 is roughly 50-60% faster than the Pi 2 which means it is ten times faster than the original Pi.

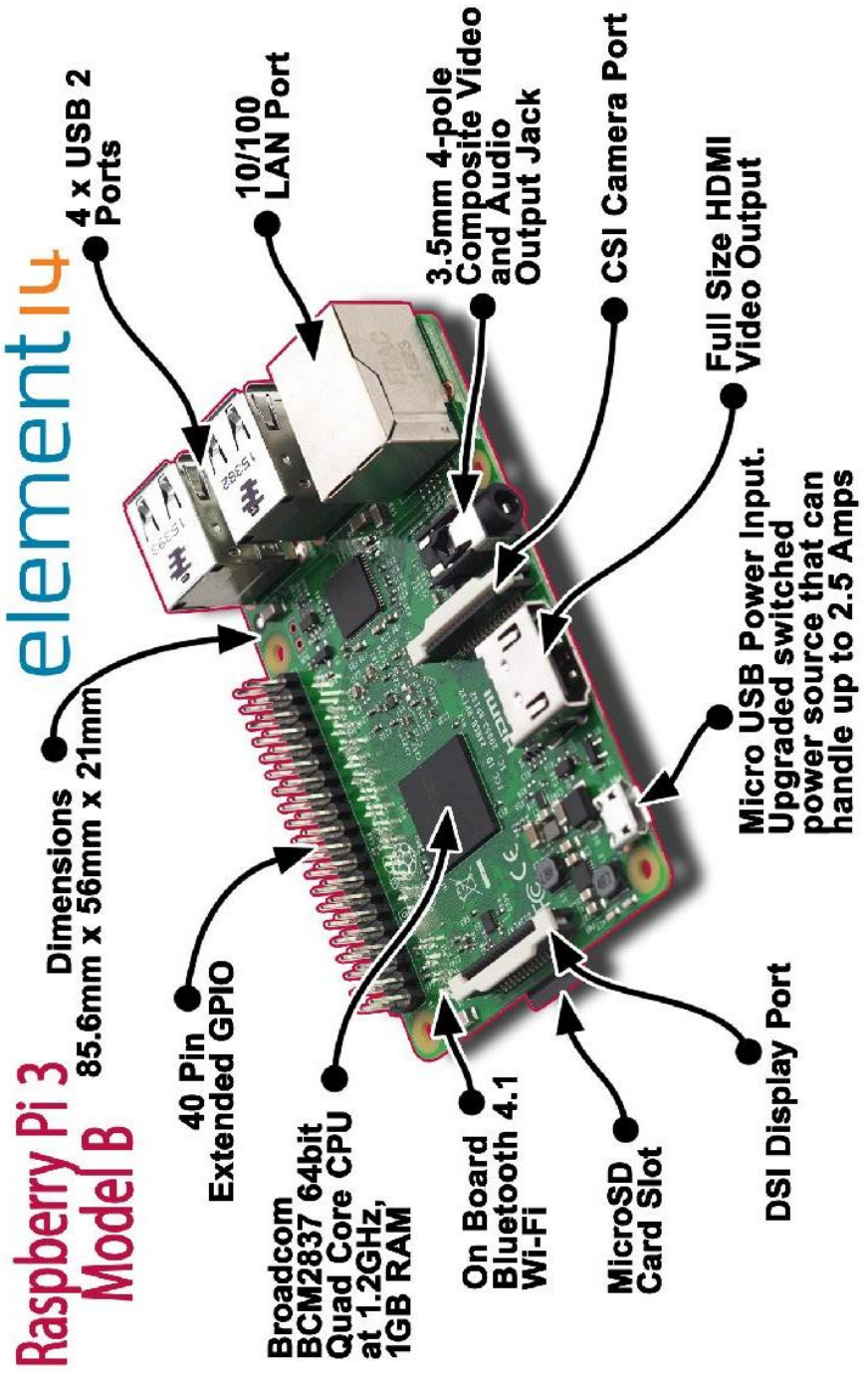
All of the connectors are in the same place and have the same functionality, and the board can still be run from a 5V micro-USB power adapter. This time round, we're recommending a 2.5A adapter if you want to connect power-hungry USB devices to the Raspberry Pi.

Raspberry Pi 3 Model B

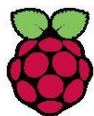


Raspberry Pi 2 Model B

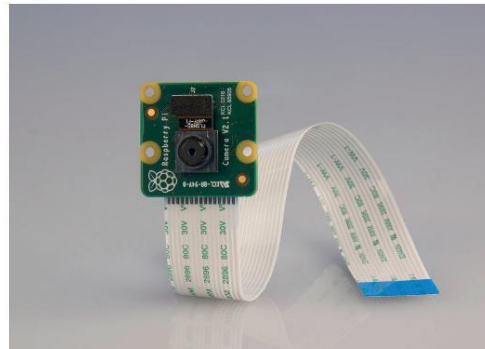




RASPBERRY PI CAMERA MODULE 2



Raspberry Pi



Camera Module

Product Name	Raspberry Pi Camera Module
Product Description	High Definition camera module compatible with all Raspberry Pi models. Provides high sensitivity, low crosstalk and low noise image capture in an ultra small and lightweight design. The camera module connects to the Raspberry Pi board via the CSI connector designed specifically for interfacing to cameras. The CSI bus is capable of extremely high data rates, and it exclusively carries pixel data to the processor.
RS Part Number	913-2664
Specifications	
Image Sensor	Sony IMX 219 PQ CMOS image sensor in a fixed-focus module.
Resolution	8-megapixel
Still picture resolution	3280 x 2464
Max image transfer rate	1080p: 30fps (encode and decode) 720p: 60fps
Connection to Raspberry Pi	15-pin ribbon cable, to the dedicated 15-pin MIPI Camera Serial Interface (CSI-2).
Image control functions	Automatic exposure control Automatic white balance Automatic band filter Automatic 50/60 Hz luminance detection Automatic black level calibration
Temp range	Operating: -20° to 60° Stable image: -20° to 60°
Lens size	1/4"
Dimensions	23.86 x 25 x 9mm
Weight	3g

www.rs-online.com/raspberrypi

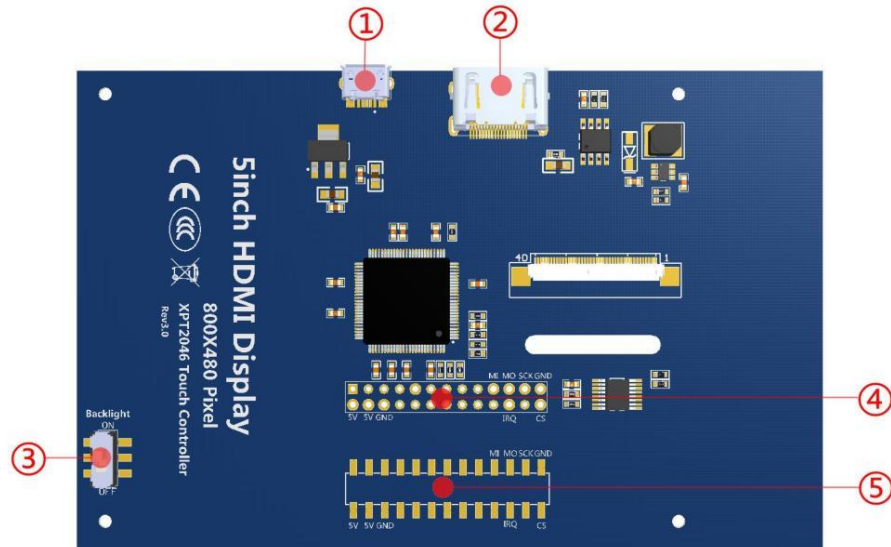


RASPBERRY PI SCREEN- 5INCH DISPLAY

【Product Parameters】

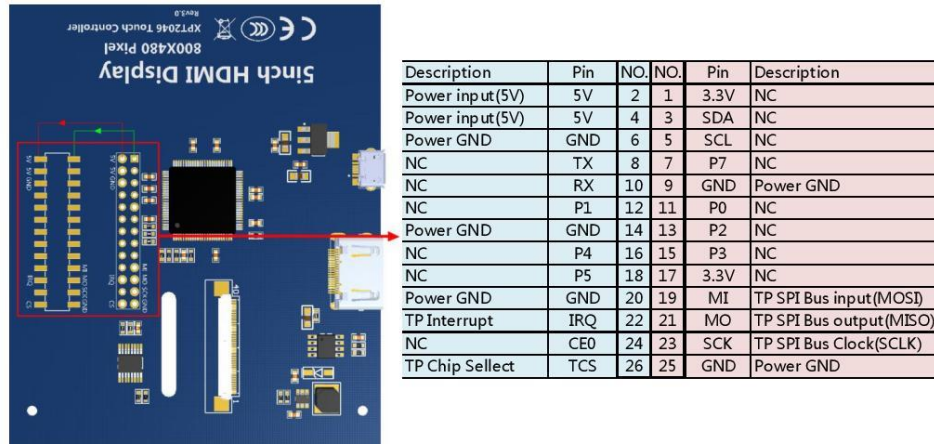
- ◆ Size: 5.0(inch)
- ◆ SKU: 6320629805
- ◆ Resolution: 800×480(dots)
- ◆ Touch: 4-wire resistive touch
- ◆ Dimensions: 121.11*77.93(mm)
- ◆ Weight: 175(g)

【Hardware Description】



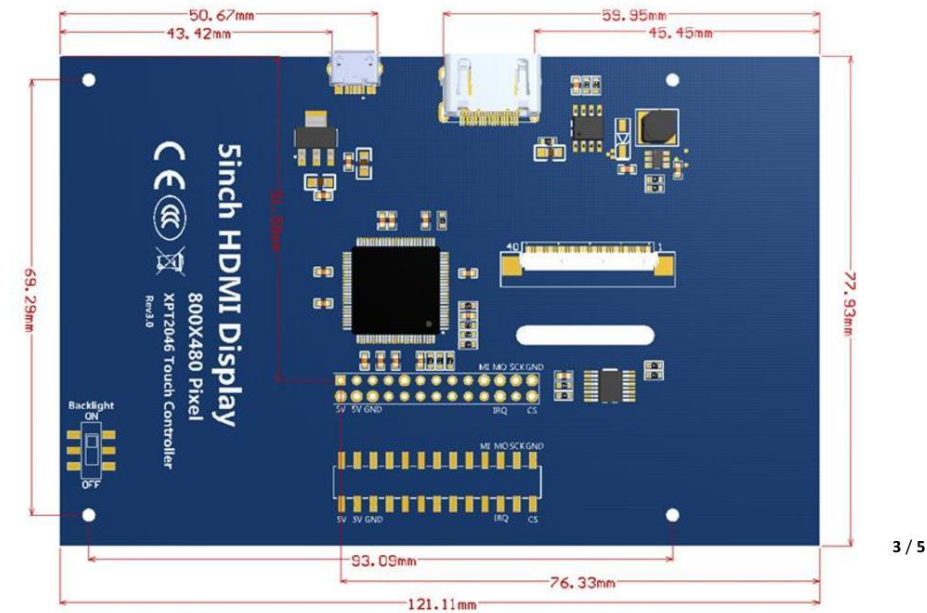
- ① USB interface: Get 5V Power from USB, If ④-13*2 Pin Socket has been connected, that this USB interface can be No Connect.
- ② HDMI interface: For HDMI transmission.
- ③ Backlight Power switch: Controls the backlight turned on and off to save power.
- ④ 13*2 Pin Socket: Get 5V Power from raspberry Pi to LCD, at the same time transfer touch signal back to raspberry Pi.
- ⑤ extended interface: extended The ④-13*2 Pin Socket signal Pin-to-Pin.

【Pin Map】



- 1)"NC" means No Connected, The Pins "NC" do not used by this LCD.
- 2)If only used for display(without touch), you can let this 13*2 Pin to be free,just connect USB and HDMI signal to make it display.
- 3) 13*2 Pin signals all extended for User.

【Dimensions】



【Connect with Raspberry Pi】

1) Connect The LCD 13*2 Pin socket to Raspberry Pi as the Picture show above.



2) Connect The LCD and Raspberry Pi with the HDMI adapter.

4 / 5

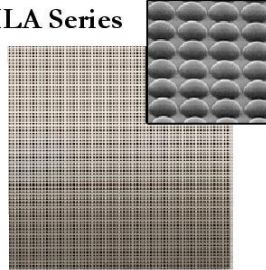
MICROLENS ARRAY

Product Specification Sheet

Microlens Arrays

THORLABS

MLA Series



Description

Thorlabs Microlens Arrays are best suited for Shack-Hartmann sensor applications. Both lenslets are made from fused silica for excellent transmission characteristics from the deep UV to IR and have a plano-convex shape that allows nearly refraction limited spots.

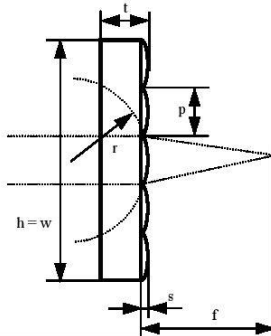
The lenses are formed using photolithographic techniques based on semiconductor processing technology, which allows for excellent uniformity in the shape and position of each microlens, unlike some microlens arrays produced from molded epoxy.

The MLA150-5C has a chrome mask that blocks light from being transmitted unless it goes through a microlens and therefore increases image contrast. The MLA150-7AR and MLA300-14AR have a broadband AR coating to reduce surface reflections in the 400-900nm spectral region to below 1%.

Specifications

Parameters	MLA150-5C	MLA150-7AR	MLA300-14AR
Substrate Material		Fused Silica (Quartz)	
Wavelength Range		From DUV to IR	
Array Size and Type		10 x 10 mm, Square Grid	
Lens Type	Round, Refractive, Plano-Convex		Square, Refractive, Plano-Convex
Lens Pitch / Diameter	150 μm / 146 μm		300 μm square
Focal Length	5.2 mm	6.7 mm	18.6 mm
AR-Coating	no	Yes, Reflectivity < 1% Within 400 ... 900 nm	
Chrome Apertures	Yes, Around Microlenses		no
Geometric Parameters			
h, w	10 mm	10 mm	10 mm
t	1.24 mm	1.19 mm	1.20 mm
p	150 μm	150 μm	300 μm
s	1.12 μm	0.87 μm	1.31 μm
r	2.380 mm	3.063 mm	8.6 mm
f	5.2 mm	6.7 mm	18.6 mm

Drawings

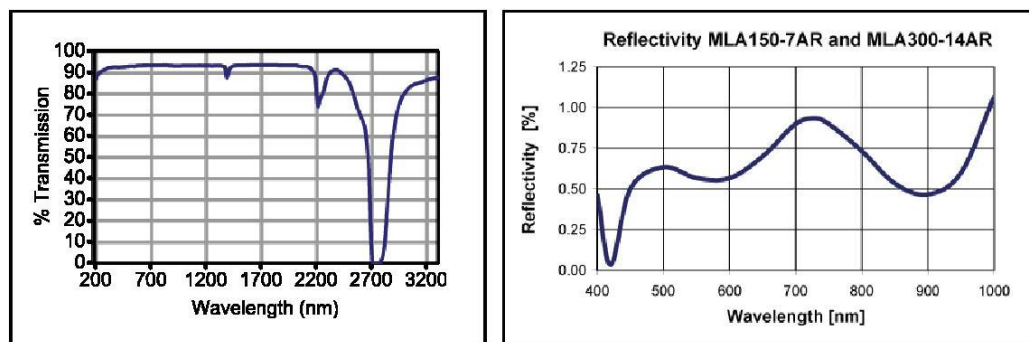


16537-02/03/2010
Specifications subject to change without notice.

Product Specification Sheet

THORLABS

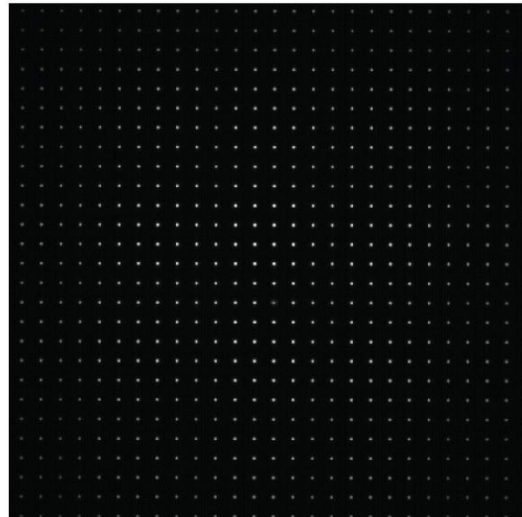
Wavelength Characteristics



Typ. Transmission of Fused Silica Material

Reflectivity including AR - Coating

Spotfield derived with the MLA150-5C Microlens Array



16537-02/03/2010
Specifications subject to change without notice.

Product Specification Sheet

THORLABS

WEEE

As required by the WEEE (Waste Electrical and Electronic Equipment Directive) of the European Community and the corresponding national laws, Thorlabs offers all end users in the EC the possibility to return "end of life" units without incurring disposal charges.

This offer is valid for Thorlabs electrical and electronic equipment

- sold after August 13th 2005
- marked correspondingly with the crossed out "wheelie bin" logo (see fig. 1)
- sold to a company or institute within the EC
- currently owned by a company or institute within the EC
- still complete, not disassembled and not contaminated

As the WEEE directive applies to self contained operational electrical and electronic products, this "end of life" take back service does not refer to other Thorlabs products, such as

- pure OEM products, that means assemblies to be built into a unit by the user (e. g. OEM laser driver cards)
- components
- mechanics and optics
- left over parts of units disassembled by the user (PCB's, housings etc.).

If you wish to return a Thorlabs unit for waste recovery, please contact Thorlabs or your nearest dealer for further information.

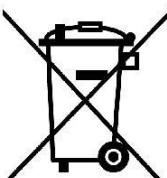
Waste Treatment on Your Own Responsibility

If you do not return an "end of life" unit to Thorlabs, you must hand it to a company specialized in waste recovery. Do not dispose of the unit in a litter bin or at a public waste disposal site.

Ecological Background

It is well known that WEEE pollutes the environment by releasing toxic products during decomposition. The aim of the European RoHS directive is to reduce the content of toxic substances in electronic products in the future.

The intent of the WEEE directive is to enforce the recycling of WEEE. A controlled recycling of end of live products will thereby avoid negative impacts on the environment.



Crossed out "wheelie bin" symbol

USA, Canada, & S. America
Thorlabs, Inc.
56 Sparta Ave
Newton, NJ 07860, USA
Tel: 973-300-3000
Fax: 973-300-3600
www.thorlabs.com
email: sales@thorlabs.com

Europe
Thorlabs GmbH
Hans-Böckler-Str. 6
85221 Dachau, Germany
Tel: +49-(0)8131-5956-0
Fax: +49-(0)8131-5956-99
www.thorlabs.com
email: Europe@thorlabs.com

UK and Ireland
Thorlabs LTD
1 Sam Thomas Place, Ely
Cambridgeshire CB7 4EX, GB
Tel: +44 (0)1353-654440
Fax: +44 (0)1353-654444
www.thorlabs.com
email: sales.uk@thorlabs.com

Scandinavia
Thorlabs Sweden AB
Bergfotsgatan 7
431 35 Mölndal, Sweden
Tel: +46-31-733-30-00
Fax: +46-31-703-40-45
www.thorlabs.com
email: scandinavia@thorlabs.com

Japan and Asia
Thorlabs Japan, Inc.
3-6-3 Kitamachi
Nerima-ku, Tokyo 179-0081, Japan
Tel: +81-3-6915-7701
Fax: +81-3-6915-7716
www.thorlabs.co.jp
Email: sales@thorlabs.jp



16537-02/03/2010
Specifications subject to change without notice.

APPENDIX E

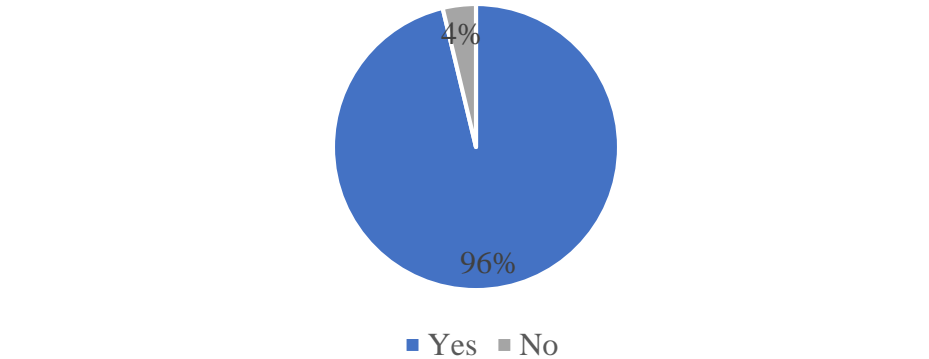
Data Gathered

The following table shows the eye check-up results of the patients' eyes in comparison to the results obtained from an autorefractometer.

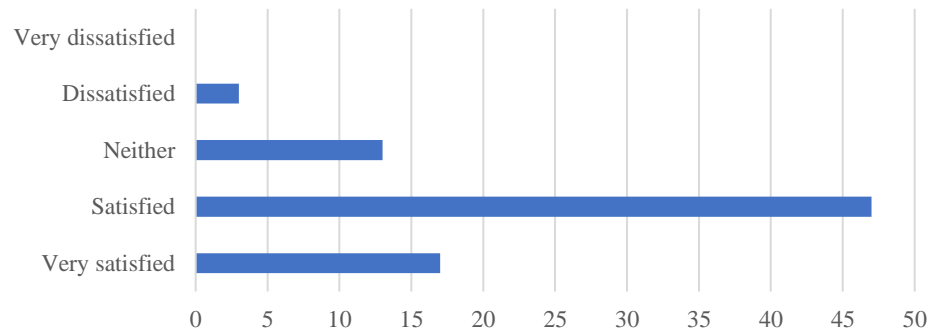
SPH		CYL		AX	
Clinical Autorefractometer	SOLLA Eye Check	Clinical Autorefractometer	SOLLA Eye Check	Clinical Autorefractometer	SOLLA Eye Check
-50	-58	-75	4	127	133
-25	-131	-25	16	150	131
25	-11	-25	0	147	121
-50	-2	-50	-1	144	81
125	-136	-100	21	132	128
25	-22	0	0	0	0
75	-105	-75	12	173	131
50	-9	0	3	0	45
-75	-20	-75	0	159	126
-25	-39	-50	5	158	124
0	-10	-50	5	109	45
50	-10	-50	-2	165	130
-25	-62	-100	6	165	130
50	-64	-75	23	149	120
100	-73	-25	7	112	131
75	-86	-25	28	123	121
25	-6	-75	1	112	52
300	-292	50	39	171	134
50	-25	-50	0	147	131
50	-146	-50	18	147	132
50	-35	-50	4	147	125
25	-36	-100	2	97	130
-50	-13	-100	0	155	120
75	-59	-25	14	123	122
75	-28	-25	0	123	132
75	-39	-75	3	152	127
50	-48	-75	10	118	122
100	-52	-25	3	112	134
100	-17	0	0	0	0
-25	-105	-100	73	165	122

The following charts show the results obtained during the survey with regard to the patients' evaluation of the prototype.

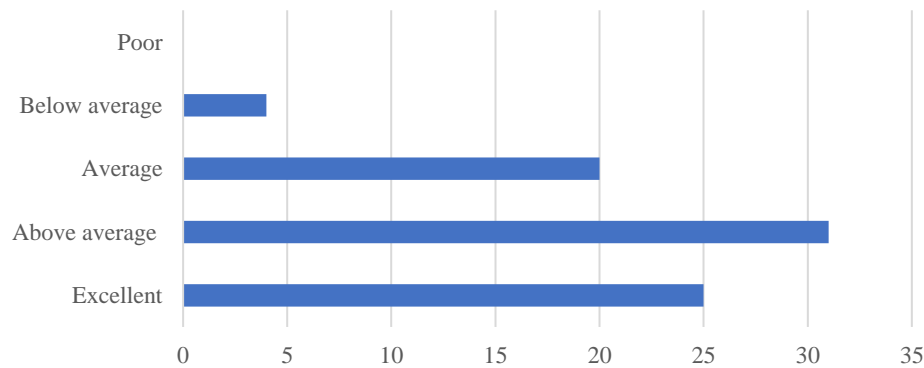
Is the device easy to use?



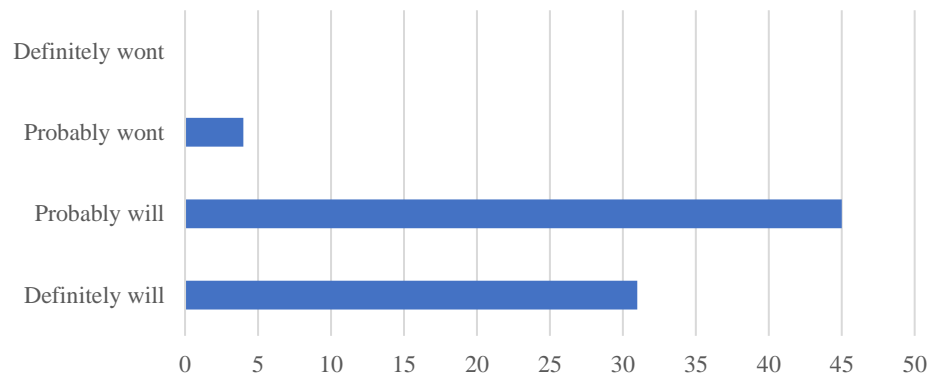
How would you rate your experience with our device?



How would you rate the performance of our device?



Will you recommend our device?



APPENDIX F

Project Manual

PROPONENTS

Atas, Marie Cattleah D.
Landicho, Larish Mariam T.
Lobo, Abigail D.
Orubia, Carla Joy L.
Silverio, Adolph Christian O.

SOLLABO

ADVISER

Engr. John Carlo V. Puno

USER MANUAL

Electronics Engineering Department
Technological University of the Philippines
Manila

Ayala Blvd., Ermita, Manila, 1000,
Metro Manila
solla.eyecheckup@gmail.com
www.sollabo.home.blog

LEGEND

- A. Switch
- B. Eye piece
- C. 4 USB ports
- D. Ethernet port
- E. LCD Screen

SAFETY AND ACCURACY

1. Don't take the eye-checkup if your eyes are tired or in a bad condition (consult your eye doctor).
2. Make sure to be on a relaxed state before and during the checkup.
3. Stay on a dark place when doing the eye-checkup.
4. Do not attempt to take the eye-checkup more than three (3) times. Take a long rest before using it again to avoid health complications.

HOW TO USE

SETUP



1. Turn ON the switch.
2. Wait for the device to boot up properly.
3. Locate the program file at the desktop shown on the screen.
4. Run the program.

EYE CHECKUP

1. Remove your eyeglass or contact lens.
2. Place your left eye on the eyecup carefully.
3. Focus on the red light.
4. Wait until the image is captured.
5. Repeat the instructions for the right eye.
6. Touch anywhere on the screen to proceed on the results.

KNOW YOUR TERMS

Spherical (SPH) - lens power needed to correct myopia or hyperopia. Minus sign (-) means you are nearsighted. Positive sign (+) means you are farsighted.

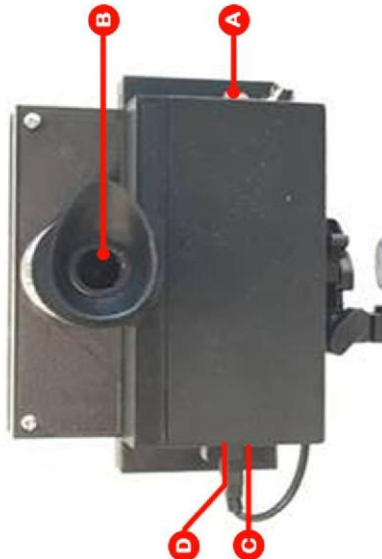
Cylindrical (CYL) - lens power needed to correct astigmatism.

Axial (AX) - describes the lens meridian that contains no cylinder power to correct astigmatism.

Myopia (nearsightedness) - occurs when light focuses before the retina, causing far objects to appear blurred.

Hyperopia (farsightedness)- occurs when light focuses beyond the retina causing near objects to appear blurred.

Astigmatism - occurs when the cornea of the eye is irregularly shaped, causing objects at any distance to be out of focus.



APPENDIX G

Letters and Certifications



TECHNOLOGICAL UNIVERSITY OF THE PHILIPPINES

Ayala Blvd., cor San Marcelino St., Ermita, Manila

Telefax No. 522-3524; <http://www.tup.edu.ph>



**COLLEGE OF ENGINEERING
ELECTRONICS ENGINEERING DEPARTMENT**

SERVICE AGREEMENT

Title of Activity: (Deployment) "SOLLABO: MEASUREMENT OF LOWER-ORDER ABERRATIONS IN THE EYES USING WAVEFRONT ABERROMETRY BASED ON A CCD CAMERA"

Description of Activity:

The "SOLLABO: MEASUREMENT OF LOWER-ORDER ABERRATIONS IN THE EYES USING WAVEFRONT ABERROMETRY BASED ON A CCD CAMERA" is a study that will construct a portable eye checkup device using wavefront aberrometry that will measure the refractive errors in the eye accurately. The study primarily focused on the measurement of the lower-order aberrations (LOA), which include myopia, hyperopia, and astigmatism.

Responsibilities of the Client:

1. Regularly maintain and ensure its functionality.
2. Regarding for any potential development to the project study the client may suggest it to the researchers from TUP.
3. The parties hereto understand that during the technology adoption, the Transferor (TUP) shall give Transferee (Client) a gratis usage for four months. After four months, a rent-to-transfer scheme shall be employed. Payments shall be made payable by the Transferee to the Transferor under this agreement under the following scheme:
 - a. Gratis usage for the first four (4) months.
 - b. Rental fee of Php 500.00 of technology adoption stage.
4. Provide the necessary information in which the project is beneficial to its client.
5. Accommodate researchers from TUP if there are further studies that will be conducted related to the transferred technology/machine/prototype/project/study.

Responsibilities of TUP:

1. Provide the device, instruction manual and necessary training to operate the machine to ensure a satisfactory turn-over to the Client.
2. Give necessary information about the limitation of the device.
3. Provide technical support in case of device malfunction.

The parties hereto agree to keep any information identified as confidential by the disclosing party confidential using methods at least as stringent as each party uses to protect its own confidential

information. "Confidential Information" shall include the Proprietor's development plan, the Option Technology and all information concerning it and any other information marked confidential or accompanied by correspondence indicating such information is confidential exchanged between the parties hereto prior to or during the Option Period.

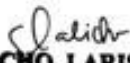
This agreement has been signed by authorized representatives of the Parties and shall enter effect upon signature by the parties.

Conforme:

**Project Proponents/Researchers
from TUP:**

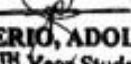

ENGR. JOHN CARLO V. PUNO
Adviser


ATAS, MARIE CATTLEAH D.
ECE 5TH Year Student

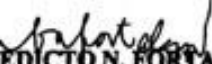

LANDICHO, LARISH MARIAM T.
ECE 5TH Year Student


LOBO, ABIGAIL D.
ECE 5TH Year Student


ORUBIA, CARLA JOY L.
ECE 5TH Year Student

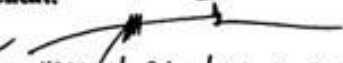

SILVERIO, ADOLPH CHRISTIAN O.
ECE 5TH Year Student

Witness: **ENGR. NILO M. ARAGO**
ENGR. LEAN KARLO S. TOLENTINO


ENGR. BENEDICTO N. FORTALEZA
Dean, College of Engineering

Date Signed: 1/30/19

Client:


HON. LUCIANA P. NOLASCO
Brgy. Captain

Witness:


JOY NABONG
Secretary


PABLITO DE SOTTO
Admin



UNIVERSITY OF SANTO TOMAS HOSPITAL
EYE INSTITUTE



March 6, 2019

This is to certify that the prototype of the research entitled "Measurement of Lower Order Aberrations in the Eyes using Wavefront Aberrometry Based on a CCD Camera" has been tested and proven safe by ophthalmologists and recommended to be used.

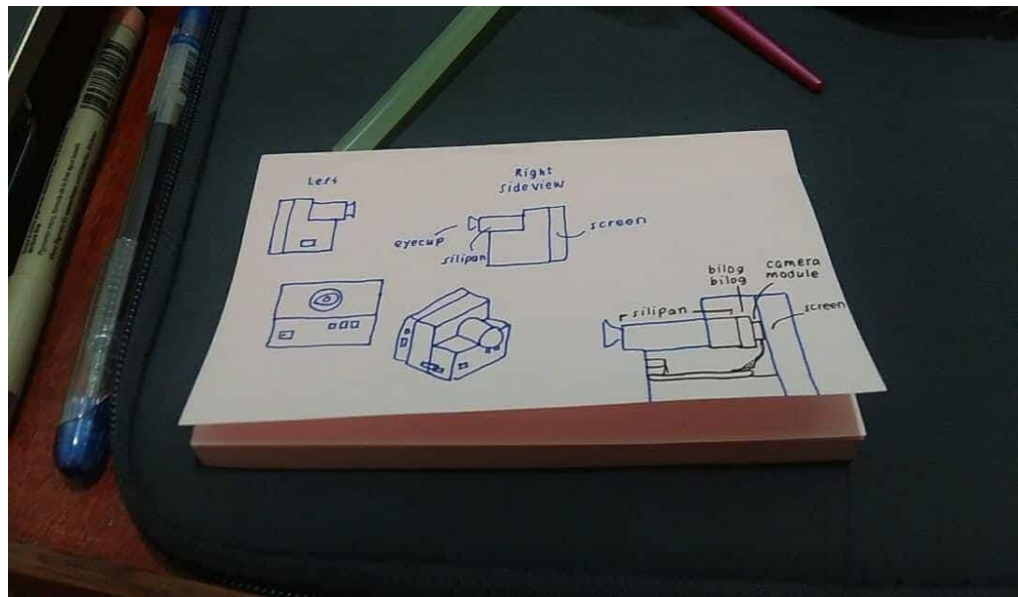
This certification is issued upon request of the proponents for research purposes only.

A handwritten signature in black ink, appearing to read "Alexander Gerard L. Gungab".

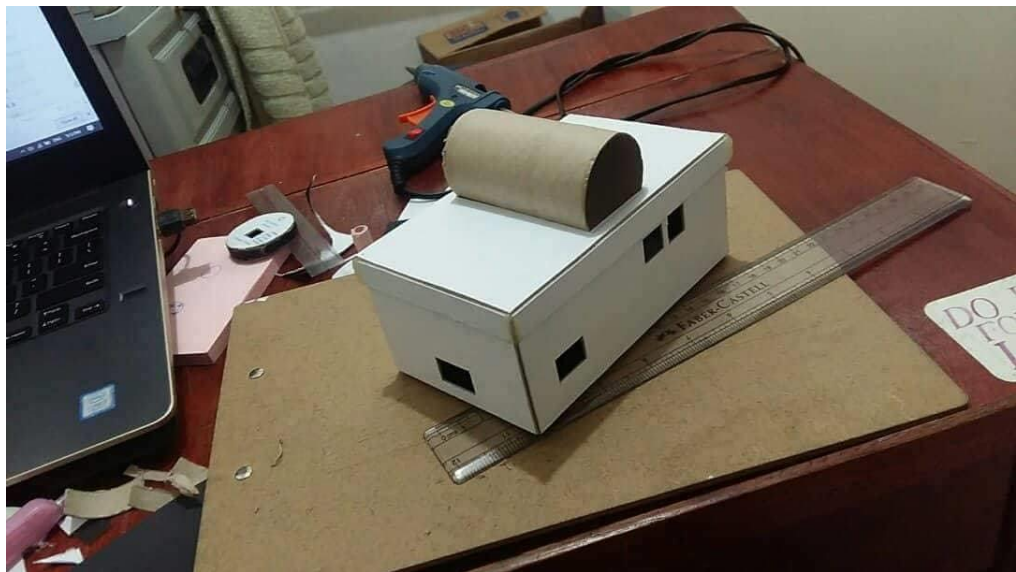
Alexander Gerard L. Gungab, MD
Assistant Chief Resident
UST Eye Institute
University of Santo Tomas Hospital

APPENDIX H

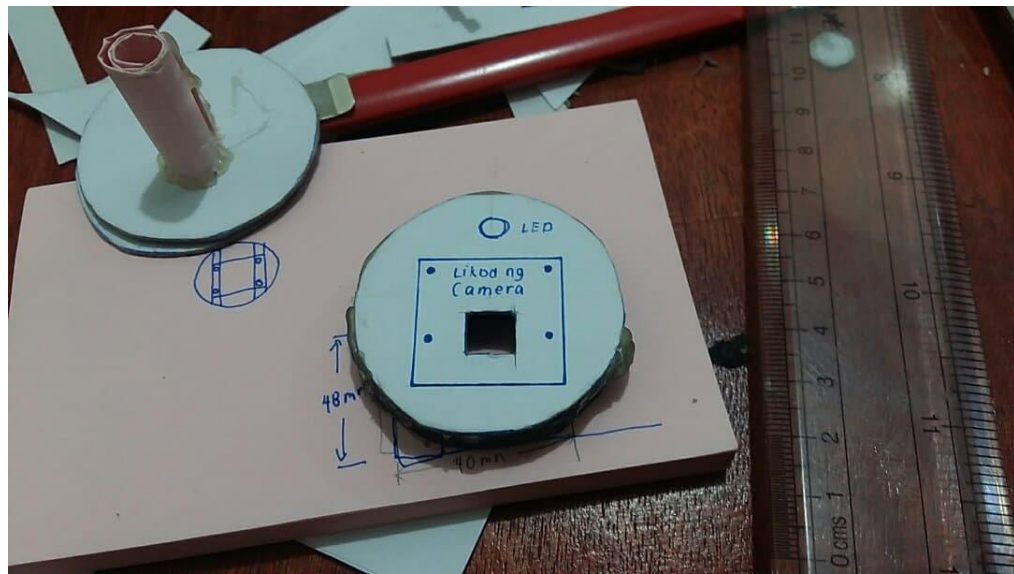
Project Documentation



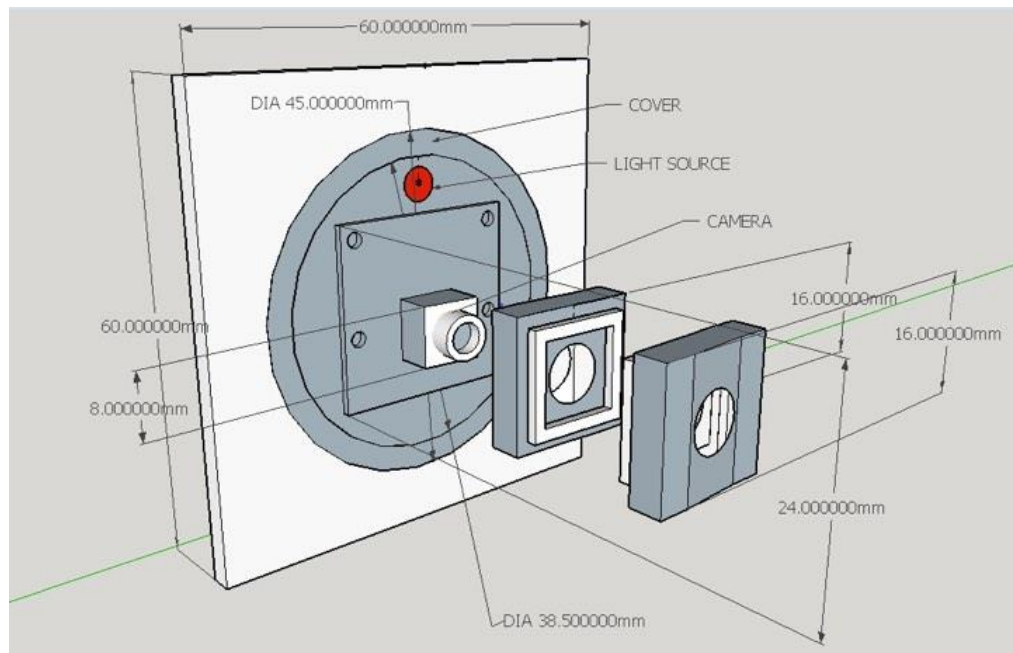
Project conceptualization



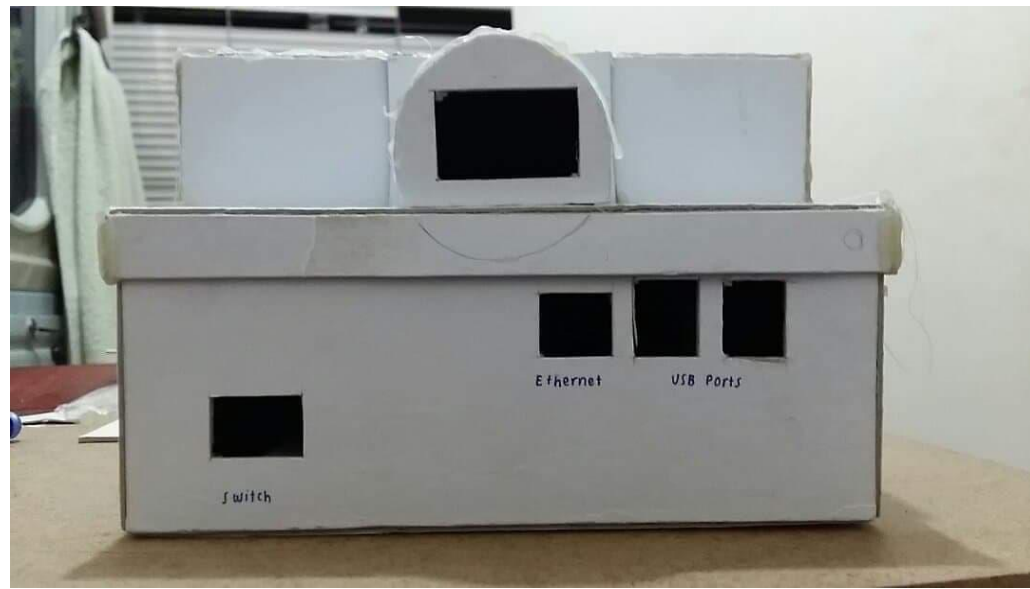
Conceptualization of the device



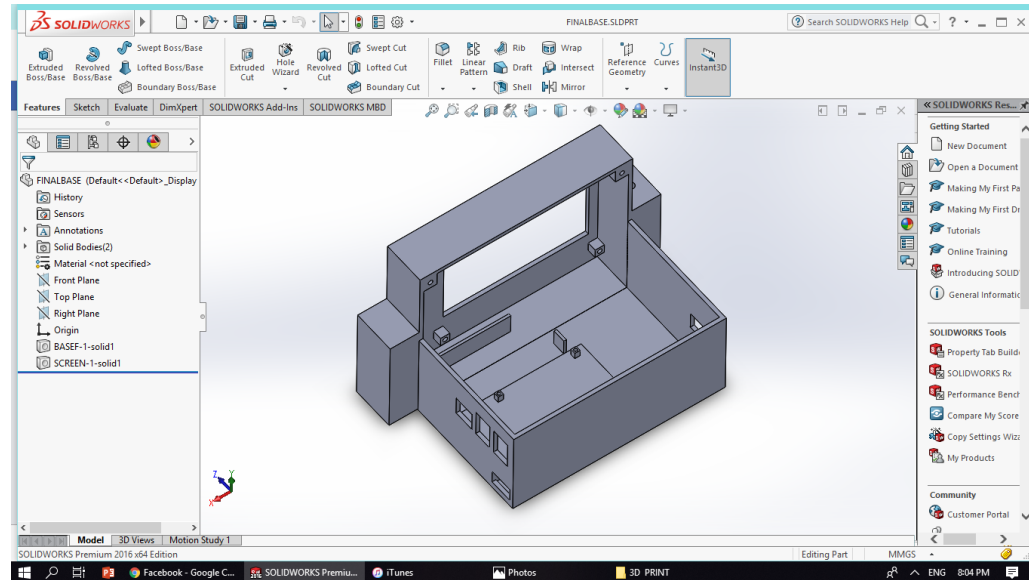
Conceptualization of lenses using card board



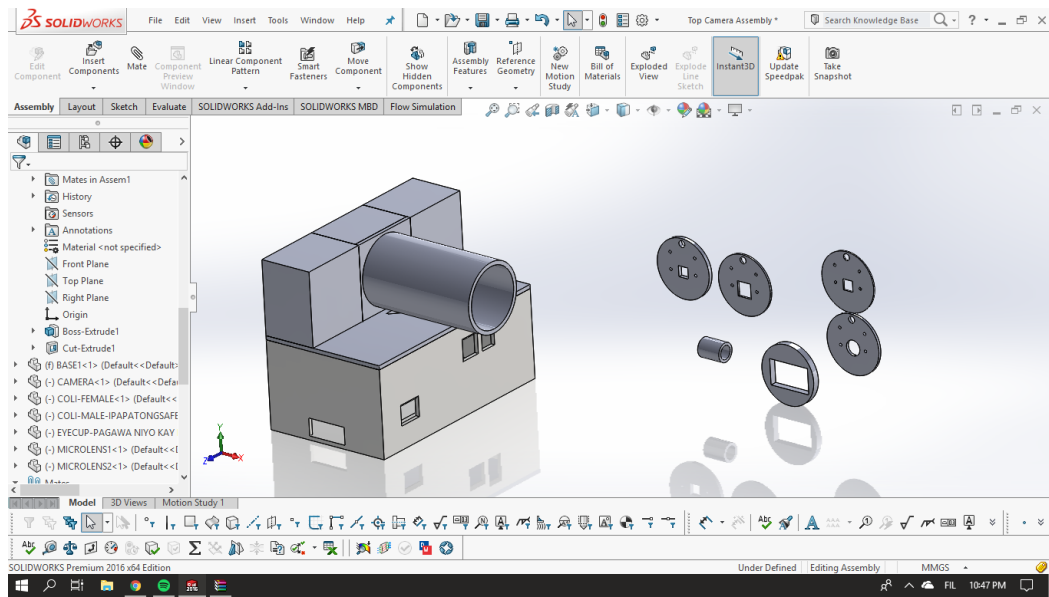
Design using Sketchup



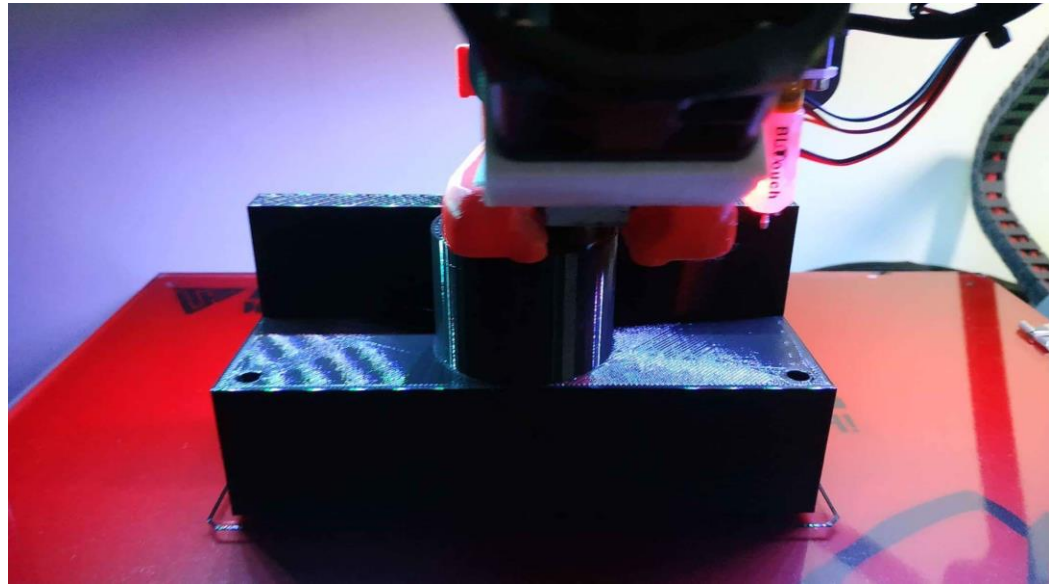
Conceptualization of the device's chassis using card board



Design using Solidworks



Design using Solidworks



3D Printing of the case



Inner View of the Prototype



Front And Back View of the Prototype



Certification at University of Santo Tomas Hospital



Project Deployment at Baranggay Paso De blas



APPRECIATE 2019: SOLLABO BOOTH



APPRECIATE 2019: SOLLABO BOOTH



TOPIC DEFENSE



TITLE DEFENSE



PROGRESS PRESENTATION



PREFINAL DEFENSE



FINAL DEFENSE

APPENDIX I

Researcher's Profile

MARIE CATTLEAH D. ATAS

Block 15 Lot 1, Gemini St., San Marino Heights, Salawag,
Dasmariñas City, Cavite, 4114
0975-718-1330
cattleahmarie@gmail.com



EDUCATION

Tertiary	TECHNOLOGICAL UNIVERSITY OF THE PHILIPPINES Bachelor of Science in Electronics Engineering Ayala Blvd. Ermita, Manila 2014-Present
Secondary	INFANT JESUS MONTESSORI CENTER Blk 22-23, San Marino City, Salawag Dasmariñas City, Cavite 2010-2014
Primary	INFANT JESUS MONTESSORI CENTER Blk 22-23, San Marino City, Salawag Dasmariñas City, Cavite 2009 – 2010
	MOUNT CARMEL SCHOOL OF CAVITE San Marino City, Salawag Dasmariñas City, Cavite 2007-2009
	JESU MARI SCHOOL San Marino City, Salawag Dasmariñas City, Cavite 2005-2007
	SHERLYN LEARNING CENTER Trece Martires City, Cavite 2004-2005

MARIE CATTLEAH DURANO ATAS

page 2

CO-CURRICULAR ACTIVITES

2014-Present	Member, Organization of Electronics Engineer Students Technological University of the Philippines-Manila
2016- 2017	Member, Institute of Electronics Engineers of the Philippines Manila Chapter

SEMINARS ATTENDED

24 November 2018	Impact and Benefits of Industry 4.0: A Smart Factory Automation by Engr. Rally G. Uminga IECEP – Manila Student Chapter, National University
	Internet of Things and Telecom: The New Golden Era by Engr. Christian P. Enoval IECEP – Manila Student Chapter, National University
	Virtual Reality of Things by Dr. Ronnie O. Serfa Juan IECEP – Manila Student Chapter, National University
27 November 2018	SYNCHRONIZE: Bridging Competent Students to the Competitive World Technological University of the Philippines
10 December 2018	Telecommunication Network Design and Rollout Collegio de San Juan de Letran
	Digital TV Systems Design and Measurement Collegio de San Juan de Letran

MARIE CATTLEAH D. ATAS

page 3

PERSONAL INFORMATION

Date of Birth : December 12, 1997
Age : 20 years old
Gender : Female

LANDICHO, LARISH MARIAM T., ECT

B5 L6 Hockey Street, Villa Olympia Phase IV
San Pedro, Laguna
+639269893179
larishmariam.landicho@tup.edu.ph



EDUCATION

Tertiary	TECHNOLOGICAL UNIVERSITY OF THE PHILIPPINES Ayala Boulevard, Ermita, Manila Bachelor of Science in Electronics Engineering 2014-Present
Secondary	SISTERS OF MARY IMMACULATE SCHOOL Father Masi St, San Antonio San Pedro, Laguna 2009-2013
PRIMARY	: INFANT JESUS MONTESSORI CENTER Camella Homes Woodhills San Pedro, Laguna 2008-2009
	AMAZING GRACE SCHOOL Baranggay San Vicente San Pedro, Laguna 2005-2008
	MATER ECCLESIAE SCHOOL Mater Ecclesiae Street, San Vicente San Pedro, Laguna 2003-2005

CO-CURRICULAR ACTIVITIES

June 2014-Present	Member, Organization of Electronics Engineering Students, Technological University of the Philippines – Manila
-------------------	--

LARISH MARIAM T. LANDICHO, ECT

page 2

June 2017- March 2018	Organization of Electronics Engineering Students Officer, General Staff College of Engineering Technological University of the Philippines
January 2017-Present	ECT Associate Member, Institute of Electronics Engineers of the Philippines

SEMINARS ATTENDED

24 November 2018	Impact and Benefits of Industry 4.0: A Smart Factory Automation by Engr. Rally G. Uminga IECEP – Manila Student Chapter, National University
	Internet of Things and Telecom: The New Golden Era by Engr. Christian P. Enoval IECEP – Manila Student Chapter, National University
	Virtual Reality of Things by Dr. Ronnie O. Serfa Juan IECEP – Manila Student Chapter, National University
27 November 2018	SYNCHRONIZE: Bridging Competent Students to the Competitive World Technological University of the Philippines
10 December 2018	Telecommunication Network Design and Rollout Collegio de San Juan de Letran
	Digital TV Systems Design and Measurement Collegio de San Juan de Letran
2 February 2019	GET LICENSED 2019 University of the Philippines

LARISH MARIAM T. LANDICHO, ECT

page 3

PERSONAL BACKGROUND

Date of Birth : April 12, 1997
Place of Birth : Lopez, Quezon
Age : 21 years old
Gender : Female

ABIGAIL D. LOBO, ECT

B41 L14 PH1 Zone 6 Mabuhay Homes 2000 Paliparan 2
Dasmariñas City, Cavite
+639298145517
abigail.lobo@tup.edu.ph



EDUCATION

Tertiary	TECHNOLOGICAL UNIVERSITY OF THE PHILIPPINES Ayala Boulevard, Ermita, Manila Bachelor of Science in Electronics Engineering DOST Scholar – RA 10612 2014-Present
Secondary	MAHONRI ACADEMY AND SCIENCE HIGH SCHOOL Phase 3 Mabuhay Homes 2000 Paliparan 2 Dasmariñas City, Cavite 2010-2014
PRIMARY :	MAHONRI ACADEMY AND SCIENCE HIGH SCHOOL Phase 3 Mabuhay Homes 2000 Paliparan 2 Dasmariñas City, Cavite 2004 – 2010

CO-CURRICULAR ACTIVITIES

June 2014-Present	Member, Organization of Electronics Engineering Students, Technological University of the Philippines – Manila
June 2016-Present	Member, DOST Scholar's Club, Technological University of the Philippines – Manila
January 2017-Present	ECT Associate Member, Institute of Electronics Engineers of the Philippines

ABIGAIL D. LOBO, ECT

page 2

SEMINARS ATTENDED

24 November 2018	Impact and Benefits of Industry 4.0: A Smart Factory Automation by Engr. Rally G. Uminga IECEP – Manila Student Chapter, National University
	Internet of Things and Telecom: The New Golden Era by Engr. Christian P. Enoval IECEP – Manila Student Chapter, National University
	Virtual Reality of Things by Dr. Ronnie O. Serfa Juan IECEP – Manila Student Chapter, National University
27 November 2018	SYNCHRONIZE: Bridging Competent Students to the Competitive World Technological University of the Philippines
10 December 2018	Telecommunication Network Design and Rollout Collegio de San Juan de Letran
	Digital TV Systems Design and Measurement Collegio de San Juan de Letran
2 February 2019	GET LICENSED 2019 University of the Philippines

PERSONAL BACKGROUND

Date of Birth :	August 6, 1997
Place of Birth :	Valenzuela City, Metro Manila
Age :	21 years old
Gender :	Female

CARLA JOY L. ORUBIA, ECT

11 Copenhagen St., Vista Verde North Executive Village,
Caybiga, Caloocan City
+639557483156
carlajoy.orubia@tup.edu.ph



ORUBIA, CARLA JOY L.

EDUCATION

Tertiary	TECHNOLOGICAL UNIVERSITY OF THE PHILIPPINES Ayala Boulevard, Ermita, Manila Bachelor of Science in Electronics Engineering 2014-Present
Secondary	ST. JOSEPH SCHOOL OF LAWANG BATOP Mulawinan St., Lawang Bato, Valenzuela City 2011-2014
	STO. NIÑO DE NOVALICHES SCHOOL 36 Buenamar St., Novaliches, Quezon City 2010-2011
PRIMARY :	ST. JOSEPH SCHOOL OF LAWANG BATOP Mulawinan St., Lawang Bato, Valenzuela City 2007 – 2010
	REGINA COELI EDUCATION CENTRE FOUNDATION Bucharest St., Vista Verde North Executive Village, Llano, Caloocan City 2004 – 2007

CO-CURRICULAR ACTIVITIES

June 2014-Present	Member, Organization of Electronics Engineering Students, Technological University of the Philippines – Manila
-------------------	--

CARLA JOY L. ORUBIA, ECT

page 2

2017-2018	Research and Extension Committee Head, Organization of Electronics Engineering Students, Technological University of the Philippines – Manila
January 2017-Present	ECT Associate Member, Institute of Electronics Engineers of the Philippines

SEMINARS ATTENDED

24 November 2018	Impact and Benefits of Industry 4.0: A Smart Factory Automation by Engr. Rally G. Uminga IECEP – Manila Student Chapter, National University
	Internet of Things and Telecom: The New Golden Era by Engr. Christian P. Enoval IECEP – Manila Student Chapter, National University
	Virtual Reality of Things by Dr. Ronnie O. Serfa Juan IECEP – Manila Student Chapter, National University
27 November 2018	SYNCHRONIZE: Bridging Competent Students to the Competitive World Technological University of the Philippines
10 December 2018	Telecommunication Network Design and Rollout Collegio de San Juan de Letran
	Digital TV Systems Design and Measurement Collegio de San Juan de Letran
2 February 2019	GET LICENSED 2019 University of the Philippines

CARLA JOY L. ORUBIA, ECT

page 3

PERSONAL BACKGROUND

Date of Birth :	November 5, 1997
Place of Birth :	Malabon City, Metro Manila
Age :	21 years old
Gender :	Female

ADOLPH CHRISTIAN O. SILVERIO, ECT

Block 8 Lot 39 Mt. Halcon Street Phase 1,
Soldiers Hills IV, Molino VI, Bacoor, Cavite
+639330540694
adolphchristian.silverio@tup.edu.ph



EDUCATION

Tertiary	TECHNOLOGICAL UNIVERSITY OF THE PHILIPPINES Bachelor of Science in Electronics Engineering Ayala Blvd. Ermita, Manila AY: 2016-Present
	TECHNOLOGICAL UNIVERSITY OF THE PHILIPPINES Electronics Engineering Technology (EsET) Carlos Trinidad Ave, Salawag, Dasmariñas, Cavite AY: 2013-2016
Secondary	SAINT FRANCIS OF ASSISI COLLEGE - Bacoor 96 Bayanan, Bacoor City, Cavite SY: 2009-2013
Primary	IMMACULADA CONCEPCION COLLEGES Phase 2, Soldiers Hills IV, Molino VI, Bacoor, Cavite SY: 2003 – 2009

CO-CURRICULAR ACTIVITIES

January 2017 - Present	Institute of Electronics Engineers of the Philippines ECT Associate Member – Manila Chapter
June 2016 – Present	Organization of Electronics Engineering Students Member College of Engineering Technological University of the Philippines – Manila

ADOLPH CHRISTIAN O. SILVERIO, ECT

page 2

SEMINARS ATTENDED

2 February 2019	Get Licensed 2019 University of the Philippines -Integrated School Auditorium (UPIS) University of the Philippines – Diliman
10 December 2018	ECE Seminar: Industry Preparedness Colegio de San Juan de Letran, Intramuros, Manila
27 November 2018	SYNCHRONIZE: Bridging Competent Students to the Competitive World Technological University of the Philippines Ayala Blvd. Ermita, Manila
24 November 2018	ACROSS BORDERS: Electronics Engineering in the Philippines and the ASEAN Economic Community National University Annex Building, Sampaloc, Manila
1 September 2018	Photoshop Workshop 2018 Technological University of the Philippines Ayala Blvd. Ermita, Manila
30 July 2018	T.R.E.N.D.S.: Topics in Research, Electronics, Networking, and Data Science Technological University of the Philippines Ayala Blvd. Ermita, Manila
17 February 2018	CAD WORKSHOP Autodesk Fusion 360 De La Salle Santiago Zobel, Ayala Alabang Village, Muntinlupa City
10 February 2018	PRIMER: Introduction to Ethical Hacking Hotel Kimberly Manila

ADOLPH CHRISTIAN O. SILVERIO, ECT

page 3

PERSONAL BACKGROUND

Date of Birth :	May 11, 1997
Place of Birth :	Quezon City, Metro Manila
Age :	21 years old
Gender :	Male